STUDIES ON MICROBIAL CONVERSION OF BIOMASS ENERGY PRESENT IN MANNAN TO ETHANOL.

A Project Report Submitted to

Anekant Education Society's
Tuljaram Chaturchand College, Baramati
(Empowered Autonomous)

Affiliated to Savitribai Phule Pune University, Pune
Academic Year 2023-2024.

under

'Seed Money for Teacher Scheme', 2023-24
PROJECT REPORT

Submitted by
Principal Investigator
DHAWAL VIDYACHANDRA DOSHI
Assistant Professor
Department of Microbiology

STUDIES ON MICROBIAL CONVERSION OF BIOMASS ENERGY PRESENT IN MANNAN TO ETHANOL.

A Project Report Submitted to

Anekant Education Society's

Tuljaram Chaturchand College, Baramati

(Empowered Autonomous)

Affiliated to Savitribai Phule Pune University, Pune

Academic Year 2023-2024.

under

'Seed Money for Teacher Scheme', 2023-24

PROJECT REPORT

Submitted by

Principal Investigator

DHAWAL VIDYACHANDRA DOSHI

Assistant Professor

Department of Microbiology

CERTIFICATE

This is to certify that the final report of minor research project under 'Seed money for teachers' entitled **"Studies on microbial conversion of biomass energy present in mannan to ethanol"** is a record of bonafide research work carried out by Mr. Dhawal V. Doshi, Associate Professor, Department of Microbiology, Tuljaram Chaturchand College, Baramati, Dist. Pune, Maharashtra. A copy of the final report of Minor Research Project has been kept in the library of college and an executive summary of the report has been posted on the website of the College.

Principal

Avinash S. Jagtap

TULJARAM CHATURCHAND COLLEGE * BARAMATI

Declaration

I hereby declare that the minor research project report entitled "**Studies on microbial conversion of biomass energy present in mannan to ethanol"** completed and written by me under the financial support of **Seed money for teachers, Tuljaram Chaturchand College, Baramati;** has not been previously published or formed the basis of any degree, diploma, research project or any other similar title.

Place: **Baramati**

Date: **31/05/2024**

Principal Investigator

(Mr. Dhawal V. Doshi)

Acknowledgement

I express the deep sense of gratitude to the Tuljaram Chaturchand College, Baramati for sanctioning the minor research project under Seed money for teacher's scheme.

I hereby, express my sincere thanks to Dr. A. S. Jagtap (Principle of Tuljaram Chaturchand College Baramati), Prof. Y. R. Mulay (IQAC, coordinator), Prof. Dr. S.T. Pawar (Head Department of Microbiology), for their overall support throughout this work. I am also very thankful of Dr. S. T. Salunke (ARC), Mr. Abhinandan B. Shah (Registrar) and Mr. Amol S. Patil (Junior Clerk) for their valuable support.

I would also like to acknowledge DST-FIST for funding to develop infrastructure and purchase instruments like UV-visible spectrophotometer which are used extensively while working on this minor research project.

Place: **Baramati**

Date: **31/05/2024**

Principal Investigator

(Mr. Dhawal V. Doshi)

INDEX

ABSTRACT

This study focuses on the isolation and identification of mannanase producing bacteria from garden soil, rhizosphere soil, compost, and goat dung. After enrichment and primary screening 13 bacteria were isolated with a clear zone around colony showing mannanase activity against locust bean gum (L.BG). Two of these 13 isolates were selected for further studies after secondary screening. These two secondary screened bacteria were identified by 16SrRNA gene sequencing and comparing it with the sequence of known bacteria. These two bacteria were identified as *Proteus mirabilis* and *Achromobacter denitrificans*. Physico-chemical factors were optimized for improved production of mannanase from each of these two bacteria were separately. Plackett-Burman design (PBD) was used for screening of factors showed that inoculum size and pH affect the production of mannanase in case of *Proteus mirabilis* while locust been gum (LBG) and pH affects production of mannanase by *Achromobacter denitrificans*. With the help of response surface methodology (RSM) these factors were optimised to produces maximum mannanase. These mananase were purified and used for saccharification of mannan and ethanol fermentation by *Saccharomyces cerevisiae* gave 1.367 – 1.642 g/L ethanol production after 24 hrs.

INTRODUCTION

Mannans are polysaccharides composed primarily of mannose units, and they are found in various biological systems, including plants, algae, and microorganisms (Yasar Yildiz and Toksoy Oner, 2014). Plant mannan is primarily found in the cell walls of certain plants, particularly in legumes and some species of palms. Mannans can exist in two main forms: galactomannans and glucomannan. Galactomannans consist of a mannan backbone with galactose side chains, while glucomannan has a more straightforward structure without these side chains (Mafa and Malgas, 2023). Mannans contribute to the structural integrity of plant cell walls. They provide rigidity and support, allowing plants to maintain their shape and resist external stresses. In some plants, mannan serves as a storage carbohydrate that can be mobilized during periods of growth or stress. This function is particularly important in seeds where mannan can be converted into sugars during germination. Mannans have hygroscopic properties that allow them to retain water. This characteristic is crucial for plants in arid environments, helping to maintain turgor pressure and overall health. Plant mannans are utilized as thickening agents and stabilizers in various food products. They improve texture and mouthfeel in items like ice cream and salad dressings. Due to their biocompatibility and biodegradability, mannan derivatives are explored for drug delivery systems (Voiniciuc, 2022).

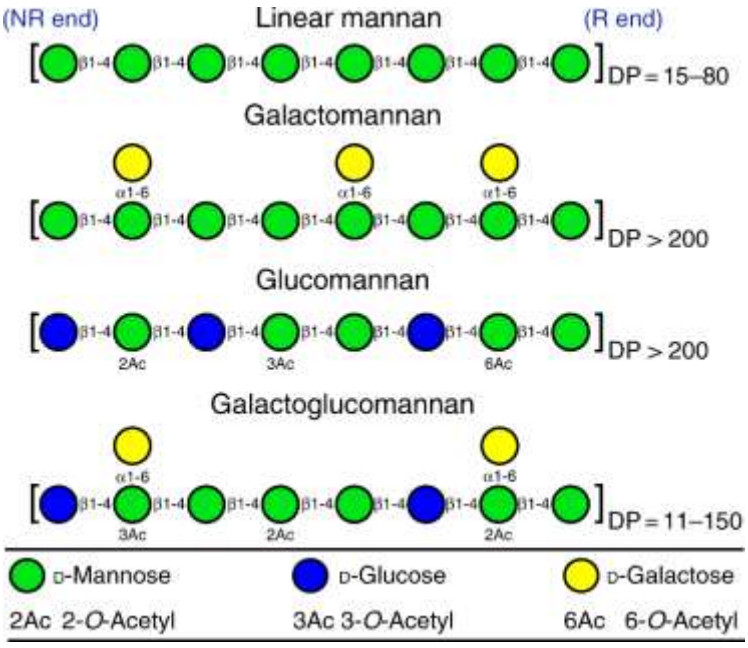

Figure 1: Structure of Mannan

Algal mannans are primarily found in certain groups of algae, particularly red algae (Rhodophyta) and brown algae (Phaeophyceae). These mannans often have unique structural features that differ from those found in terrestrial plants. In algae, mannans contribute to the composition of cell walls, providing flexibility and strength necessary for survival in aquatic environments. Algal mannans play a role in nutrient absorption from the surrounding water. Their structure allows for efficient uptake of minerals and organic compounds. Some algal species utilize mannans to form biofilms on surfaces submerged in water. This biofilm formation can influence microbial communities and nutrient dynamics in aquatic ecosystems. Algal mannans can be employed in bioremediation processes to absorb heavy metals and other pollutants from water bodies. Extracts from algal mannans are used as food additives due to their gelling properties, enhancing the texture of various food products (Kraan, 2012).

Microbial mannans are produced by a variety of microorganisms, including bacteria and fungi. These mannans can vary significantly in structure depending on the species producing them. Microbial mannans play a vital role in the decomposition of organic matter, contributing to nutrient cycling within ecosystems (Van den Abbeele, 2020). Some microorganisms produce mannans as part of their defense mechanisms against pathogens. The polysaccharides can inhibit the growth of competing microorganisms or protect against predation. Certain fungi form symbiotic relationships with plants through mycorrhizal associations, where microbial mannans facilitate nutrient exchange between the host plant and the fungus. Microbial mannans are utilized in various biotechnological applications, such as enzyme production for industrial processes. Mannan-based products are used as soil amendments to enhance soil health and promote plant growth by improving nutrient availability (Mpofu *et al*, 2007).

Table 1: Comparative analysis of different mannans.

Feature	**Plant Mannans**	**Algal Mannans**	**Microbial Mannans**
Source	Terrestrial Plants	Aquatic Algae	Bacteria/Fungi
Primary Function	Structural integrity	Nutrient absorption	Decomposition

Structural Variability	Galactomannans & glucomannan	Diverse structures	Highly variable
Industrial Applications	Food, pharmaceuticals	Bioremediation, food additives	Biotechnology, agriculture

Microbial mannanases

Mannanases are enzymes that catalyze the hydrolysis of mannan, a polysaccharide composed primarily of mannose units. These enzymes are crucial for the degradation of plant cell walls, where mannan is a significant structural component. Produced predominantly by microorganisms, mannanases have gained considerable attention in various industrial applications, including food processing, animal feed, textiles, and biofuels (Chauhan *et al.*, 2012).

Structure and Classification

Mannan is a polysaccharide primarily composed of β-(1→4)-linked mannose units. The structure can vary significantly based on the source, with different types of mannans such as glucomannans and galactomannans present in various plant tissues. The complexity and heterogeneity of mannan structures necessitate specific enzymes for their degradation (Malgas *et al.*, 2015).

Mannanases are classified based on their action on mannan substrates:

Endo-mannanases: These enzymes cleave internal β-(1→4) bonds within the mannan chain, leading to the formation of shorter oligosaccharides. They are primarily found in glycoside hydrolase (GH) families such as GH5 and GH26.

Exo-mannanases: These enzymes act on the terminal ends of mannan chains, releasing mannose or mannooligosaccharides. They are commonly classified under GH2 and GH3 families.

The classification is further refined by the CAZy (Carbohydrate-Active enZYmes) database, which categorizes mannanases based on their sequence homology and enzymatic mechanisms (Morreira, 2008).

Mechanism of Action

The catalytic action of mannanases involves a two-step process:

Substrate Binding: The enzyme binds to the mannan substrate through specific interactions between amino acid residues in the active site and the sugar moieties of mannan.

Catalytic Hydrolysis: The enzyme catalyzes the hydrolysis reaction by breaking the glycosidic bond. This action typically involves an acid-base mechanism where specific amino acids (such as glutamic acid or aspartic acid) act as proton donors or acceptors during the reaction.

The efficiency of mannanases can be influenced by various factors including pH, temperature, and substrate concentration (Songsiriritthigul *et al.*, 2011).

Sources of Mannanases

Mannanases are produced by a diverse array of microorganisms:

Bacterial Sources: Several bacterial strains are known to produce mannanases.

Bacillus spp.: These bacteria are often used in industrial enzyme production due to their ability to secrete large amounts of extracellular enzymes.

Pseudomonas spp.: Known for their versatility in degrading complex organic materials.

Streptomyces spp.: Actinomycetes that produce a variety of hydrolytic enzymes including mannanases.

Bacterial mannanases are typically extracellular and can function across a broad range of pH and temperature conditions (Dawood and Ma, 2020).

Fungal Sources: Filamentous fungi are significant producers of mannanases.

Aspergillus spp.: Commonly used in industrial applications due to their high enzyme secretion levels.

Trichoderma spp.: Known for their robust enzyme production capabilities.

Fungi generally produce a more diverse range of mannan-degrading enzymes compared to bacteria.

Other Sources: While microbial sources dominate, plant and animal-derived mannanases have also been reported. However, microbial enzymes are preferred for industrial applications due to their higher yields and specific activity profiles (Dawood and Ma, 2020).

Production Conditions

The production of microbial mannanases can be optimized through various conditions:

Substrate Selection -

The choice of carbon source is critical for maximizing enzyme yield. Common substrates include:

Lignocellulosic biomass: Such as agricultural residues that contain high levels of mannans.

Pure polysaccharides: Like guar gum or locust bean gum can also be used as substrates for enzyme production (Dawood and Ma, 2020).

Environmental Conditions -

Factors such as pH, temperature, and incubation time significantly influence enzyme production:

pH: Most bacterial mannanases exhibit optimal activity at neutral to slightly alkaline pH (6-8), while fungal enzymes may perform better under acidic conditions (pH 4-5).

Temperature: The optimal temperature varies among different species; however, many microbial mannanases show activity at temperatures ranging from 30°C to 60°C (Dawood and Ma, 2020).

Fermentation Techniques -

Both submerged fermentation (SmF) and solid-state fermentation (SSF) techniques can be employed for enzyme production:

SmF: Provides better control over environmental conditions but may result in lower yields compared to SSF.

SSF: Often yields higher amounts of enzymes due to the natural growth conditions mimicking those found in nature (Dawood and Ma, 2020).

Applications of Mannanases

Mannanases have diverse applications across several industries:

Food Industry

In food processing, mannanases improve texture and quality in products like baked goods and dairy items by breaking down complex polysaccharides such as guar gum and locust bean gum. This enzymatic treatment enhances dough properties and stability while reducing viscosity.

Animal Feed

Mannanases are used in animal feed formulations to improve nutrient digestibility by breaking down non-starch polysaccharides in feed ingredients like soybean meal. This leads to better nutrient absorption and overall growth performance in livestock (Latham *et al.*, 2018).

Textile Industry

In textile processing, mannanases help remove impurities from natural fibers like cotton. Their use reduces reliance on harsh chemicals, leading to more environmentally friendly processing methods (Mojsov, 2011).

Biofuel Production

In biofuel production from lignocellulosic biomass, mannanases play a crucial role in degrading hemicellulose components within plant cell walls. This action enhances cellulose accessibility for fermentation processes, ultimately improving biofuel yields (Zhang, 2019).

Pharmaceuticals

Mannanases have potential applications in pharmaceuticals for drug delivery systems where polysaccharides serve as carriers. Their ability to degrade specific polysaccharides can be harnessed for controlled release formulations (Galli and Tsai, 2012).

Paper and Pulp Industry

In the paper industry, mannanases assist in breaking down hemicellulosic components during pulping processes, improving fiber separation and reducing chemical usage (Yang *et al.*, 2017).

Biotechnological Advances

Recent advancements have significantly improved the production and application potential of microbial mannanases:

Genetic Engineering

Recombinant DNA technology allows for the engineering of microbial strains that produce modified versions of mannanases with enhanced properties such as increased thermostability or altered substrate specificity.

Immobilization Techniques

Enzyme immobilization on various supports enhances stability and reusability in industrial applications. This process allows for continuous operation in bioreactors while reducing costs associated with enzyme replacement.

Environmental Impact

The use of microbial mannanases is considered environmentally friendly due to their biodegradability and lower toxicity compared to synthetic chemicals. Their application in waste treatment processes effectively degrades organic matter while contributing to sustainable practices across industries (Dawood and Ma, 2020).

Future Perspectives

The future research directions for microbial mannanases include:

1. Exploration of Novel Sources: Investigating less-studied microorganisms from extreme environments may yield novel enzymes with unique properties suitable for specific industrial applications.

2. Enzyme Engineering: Continued advancements in protein engineering techniques could lead to the development of highly efficient mannanase variants tailored for specific industrial processes.

3. Sustainable Practices: Emphasizing eco-friendly approaches in enzyme production will align with global sustainability goals while enhancing industrial efficiency.

4. Integration into Biorefineries: Incorporating mannanase applications into biorefinery processes could optimize resource utilization from biomass while producing value-added products.

Microbial mannanases represent a significant area of research with vast industrial applications spanning food processing, animal feed formulation, textiles, biofuels, pharmaceuticals, and more. Their ability to hydrolyze complex polysaccharides makes them invaluable tools across diverse fields. Ongoing research into their mechanisms of action, optimization methods for production processes, and exploration of novel applications will continue to enhance their utility across various sectors.

AIMS AND OBJECTIVES

- To isolate, identify and characterize mannan degrading microorganisms.
- Production of fermentable sugar and second-generation ethanol from mannan.

MATERIALS AND METHODS

Collection of samples

Garden soil

A trowel was used to scrape off the top layer (about 1-2 cm) of soil to eliminate contaminants such as leaves or debris. Soil was dug down to a depth of about 5-15 cm, to collect soil from multiple spots within the chosen area to create a composite sample. Collected soil was transferred into a sterile container and sealed to prevent contamination (Phothichitto *et al.*, 2006).

Location coordinates:

Tuljaram Chaturchand College of Arts, Science and Commerce (TCC), Baramati

5H5J+X25, Baramati, Maharashtra 413102, India

Lat-18.159728o

Long-74.580293o

Rhizosphere soil

Soil was carefully dug around the root system of the plant, taking care not to damage the roots. Aim for a depth was of about 5–15 cm. Soil from several points around the root zone was collected to ensure capturing the rhizosphere effect adequately. Sterile spatula was used to transfer the collected soil into your sterile container (Rosariastuti *et al.*, 2022).

Location coordinates:

Tuljaram Chaturchand College of Arts, Science and Commerce (TCC), Baramati

5H5J+X25, Baramati, Maharashtra 413102, India

Lat-18.15978o

Long-74.58035o

Compost sample

Surface debris such as leaves or twigs were removed to expose the compost material underneath. A trowel was used to dug the compost pile for a depth of about 10-20 cm. Collected compost sample was transferred into a sterile container.

Location coordinates:

Katewadi, Maharashtra, India

4MM4+F23, Katewadi, Maharashtra 413102, India

Lat-18.132924o

Long-74.655048o

Goat Dung

Goat dung contain protein organic acid, cellulose, aliphatics and organic matter contain is higher other livestock manure. Goat dung was collected in sterile bag by wearing sterile hand gloves.

Location coordinates:

Lat-18.132924o

Long-74.655048o

Enrichment of Mannanase producing microorganisms

In order to specifically promote the development of bacteria that produce mannanase, 1 gram or 1 milliliter of the sample was dissolved in 10 milliliters of sterile 0.8% normal saline and combined using a vortex. A one percent (v/v) portion of the mixture was added to twenty milliliters of enrichment medium, which was altered from Abe et al., 1994. The broth is incubated for 18 to 24 hours at 30 degrees Celsius while being shaken at 150 revolutions per minute.

The composition of the enrichment medium included (w/v):

0.1% yeast extract

0.1% polypeptone

0.1% ammonium nitrate (NH_4NO_3)

0.14% potassium dihydrogen phosphate (KH_2PO_4)

0.02% magnesium chloride ($MgCl_2$)

Additionally, 1% locust bean gum (LBG) served as the primary carbon and energy source in the medium (Rattanasuk and Ketudat-Cairns, 2009).

Isolation of Mannanase producing bacteria

Mannanase-producing bacteria were isolated from overnight-grown enrichment broths. On an agar medium containing 0.5% yeast extract, 1% NaCl, 0.5% locust bean gum (LGB), 1% tryptone, 0.05% trypan blue, and 1.5% agar, a suitable dilution of the enhanced culture broth was disseminated. following a 24-hour incubation at $30^{O}C$. For additional research, the colonies exhibiting a distinct zone of mannanase activity against LBG were collected and kept on Luria-Bertani agar slants (Cheng *et al.*, 2016).

Screening of Mannanase producing bacteria

The mannanase activity of each isolate was assessed for the primary screening by measuring the diameter of the clear zone that developed. For secondary screening, the bacterial cultures with the biggest hydrolytic halo were chosen (Cheng *et al.*, 2016).

Every active isolate that had been previously screened was produced as an inoculum for secondary screening by cultivating it in 20 milliliters of Luria-Bertani broth in an aerobic environment while being shaken at 150 rpm and $30^{O}C$ for a whole day. Next, one milliliter (v/v) of each inoculum was added to 100 milliliters of enzyme production medium. In a 500-milliliter flask, 0.1% yeast extract, 0.1% polypeptone, 0.1% NH_4NO_3, 0.14% KH_2PO_4, 0.02%; $MgCl_2$ with 1% locust bean gum (LBG) were cultivated for 24 hours at 30 degrees Celsius. Centrifugation was used to remove the cells for 15 minutes at $4^{O}C$ and 9,000 rpm. To measure the mannanase activity against locust bean gum (LBG), the supernatant was collected. Enzyme activity was measured using DNSA method (Titapoka *et al.*, 2008).

Identification of bacterial cultures

Two bacterial isolates were showing maximum enzymatic activity were screened for further studies.

Uncontaminated culture plates that passed quality control were utilized to isolate 1-2 well-separated colonies. These colonies were suspended in 50 µL of Molecular Biology Grade Water and mixed thoroughly. The suspension was then incubated for 10 minutes at 95°C before being briefly centrifuged. The resulting supernatant from the lysate was employed as a template for PCR amplification using the universal primers 16S27F (5'-CCA GAG TTT GAT CMT GGC TCA G-3') and 16S1492R (5'-TAC GGY TAC CTT GTT ACG ACT T-3'), as described by Weisburg *et al.* (1991).

The amplified PCR product underwent purification through salt precipitation and was subsequently subjected to cycle sequencing using BDT v3.1 chemistry. This was followed by sequencing on an ABI 3500XL Genetic Analyzer. Additional internal primers were utilized to obtain a nearly full-length sequence, ensuring high-quality base reads that encompassed the target region. The .ab1 trace files generated post-sequencing were manually curated, converted into a FASTA read file, and assembled into a contiguous sequence, which was then exported as a FASTA file.

The consensus sequence was then subjected to a database search against the SILVA database v138 (Quast *et al.*, 2012) using the BLAST tool (Altschul *et al.*, 1990). For phylogenetic analysis, up to ten closely related neighbor sequences from different taxa were retrieved from the top 1000 hits with the highest similarity in the search results and aligned using the MUSCLE aligner (Edgar, 2004). The multiple sequence alignment was manually reviewed and used to create a consensus phylogram utilizing either the maximum likelihood or neighbor-joining algorithm with 1000 iterations (Nguyen *et al.*, 2014) via MEGA11 software (Molecular Evolutionary Genetic Analysis, version 11) (Tamura, Stecher, and Kumar, 2021).

To explore the evolutionary relationships among groups of organisms, a phylogenetic tree visually represents these connections. Each branch of the tree corresponds to a taxon being compared. Branches that emerge from a common point, known as a node, indicate taxa that have diverged from a shared ancestor. Phylogenetic trees can be either rooted or unrooted; a common root signifies the most ancestral taxon from which all taxa in the tree likely evolved. Generally, the length of the branches is crucial for

determining the evolutionary distance between two organisms. Therefore, when discussing tree topology, branch lengths are more significant than their vertical arrangement.

The horizontal lines represent branches that illustrate evolutionary lineages over time. Longer branches in the horizontal dimension indicate greater genetic change. The numerical values at the nodes represent bootstrap values in percentage terms, reflecting how often branches were replicated with the same arrangement during iterations. Consequently, higher bootstrap values indicate greater confidence in those branches. The phylogenetic relationship of the submitted organism is illustrated through a consensus phylogenetic tree. Each branch of this tree corresponds to an organism identified in the BLAST results as a relative of the submitted organism.

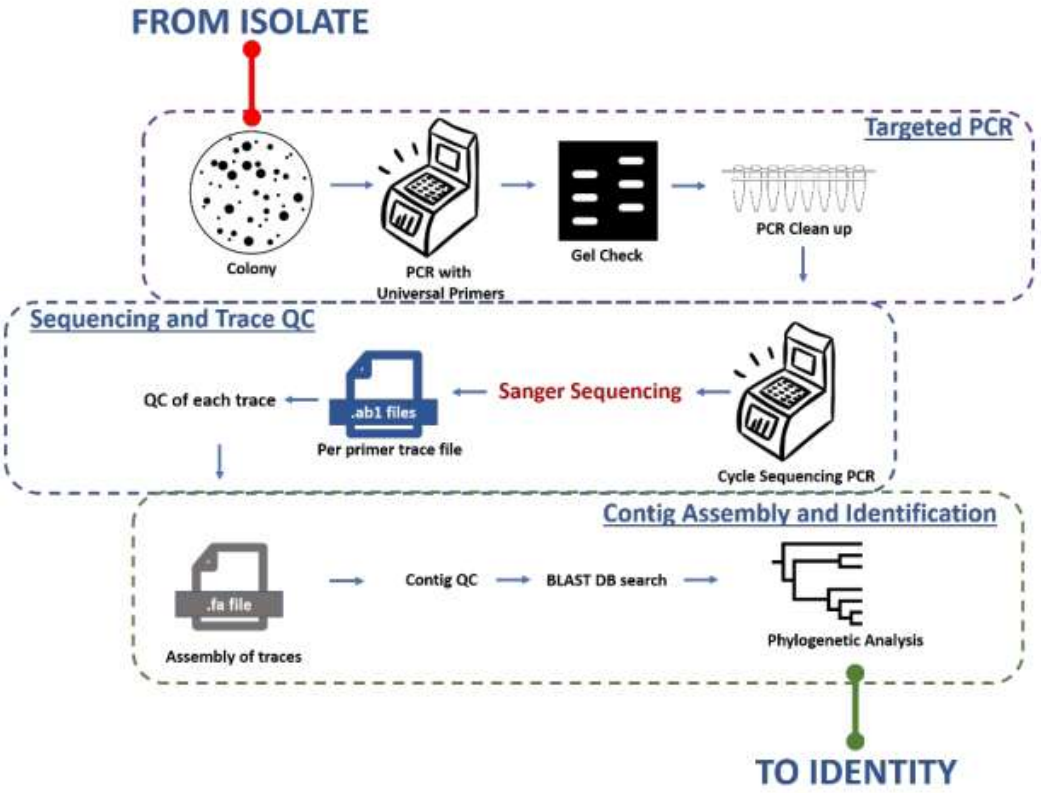

Figure 2: Steps to identify bacterium at molecular level.

Optimization of mannanase production from *Proteus mirabilis* and *Achromobacter denitrificans*

Plackett-Burman Design: Using this process, the significant factors were identified and prioritized so that the best values could be found by doing a more thorough investigation into each (Elsayed *et al.*, 2020).

Design Summary

Factors: 8
Replicates: 1
Base runs: 13
Total runs: 13
Base blocks: 1
Total blocks: 1
Center points: 1

Table 2: Design Table (randomized)

Run	Blk	A	B	C	D	E	F	G	H
1	1	-	+	+	-	+	-	-	-
2	1	-	-	-	+	+	+	-	+
3	1	+	-	+	+	-	+	-	-
4	1	+	+	-	+	+	-	+	-
5	1	+	-	-	-	+	+	+	-
6	1	-	+	+	+	-	+	+	-
7	1	-	+	-	-	-	+	+	+
8	1	+	-	+	-	-	-	+	+
9	1	+	+	-	+	-	-	-	+
10	1	+	+	+	-	+	+	-	+
11	1	-	-	+	+	+	-	+	+
12	1	-	-	-	-	-	-	-	-
13	1	0	0	0	0	0	0	0	0

Table 3: Description of factors

Factor	Name
A	LBG
B	Y. E.
C	(NH4)2SO4
D	K2HPO4
E	Na2HPO4
F	pH
G	Temp
H	Incoculum size (%)

RSM, or response surface methodology: In creating a medium for the best possible growth of organisms producing a high yield, it's crucial to consider not just the variety of elements but also their amount. A statistical experiment design that made use of data on the number of different variables screened using the Plackett-Burman technique was created using Minitab software. The yield of the product when a certain amount of different variables is applied is the response in this case. Here, the amounts of different factors were combined mathematically to determine their effects. The results were displayed, and a model was created that allows one to anticipate the number of variables needed for the medium optimization (Elsayed *et al.*, 2020).

Central Composite Design for *Proteus mirabilis*:

Design Summary

Factors: 2
Replicates: 1
Base runs: 13
Total runs: 13
Base blocks: 1
Total blocks: 1
$\alpha = 2$
Two-level factorial: Full factorial

Point Types

Cube points: 4
Center points in cube: 5
Axial points: 4
Center points in axial: 0

Table 4: Design Table

Run	Blk	A	B
1	1	-1	-1
2	1	1	-1
3	1	-1	1
4	1	1	1
5	1	-2	0
6	1	2	0
7	1	0	-2
8	1	0	2
9	1	0	0
10	1	0	0
11	1	0	0

12	1	0	0
13	1	0	0

Central Composite Design for *Achromobacter denitrificans*:

Design Summary
Factors: 2
Replicates: 1
Base runs: 13
Total runs: 13
Base blocks: 1
Total blocks: 1
$\alpha = 2$
Two-level factorial: Full factorial

Point Types
Cube points: 4
Center points in cube: 5
Axial points: 4
Center points in axial: 0

Table 5: Design Table

Run	Blk	A	B
1	1	-1	-1
2	1	1	-1
3	1	-1	1
4	1	1	1
5	1	-2	0
6	1	2	0
7	1	0	-2
8	1	0	2
9	1	0	0
10	1	0	0
11	1	0	0
12	1	0	0
13	1	0	0

Purification of mannanase enzyme

The crude enzyme was centrifuged at 5000 rpm for 20 minutes. The sample was then transferred to a beaker containing a stir bar and placed on a magnetic stirrer. While the sample was stirring, saturated ammonium sulfate was slowly added to achieve a final concentration of 80% saturation. The volume of ammonium sulfate needed was equal to the volume of the sample. Adding the ammonium sulfate very slowly ensured that

the local concentration around the addition site did not exceed the desired salt concentration.

Once the total volume of ammonium sulfate was added, the beaker was moved to 4°C for overnight. The mixture was then transferred to a centrifuge tube, and the precipitate was centrifuged at 5000 rpm for 20 minutes. The supernatant was carefully removed and discarded. The pellet was re-suspended in phosphate buffer solution (PBS). Finally, enzyme activity and total protein were determined (Katoch, 2011).

Second generation ethanol production.

For the fermentations in the presence of purified enzymes, β-mannanase extracted from production media (500 U) was added into YPA fermentation media containing 5 g/L 1,4-β-d-mannan, and cultivation of Saccharomyces cerevisiae was initiated. The concentrations of ethanol in the fermentation media was determined (Ishii *et al.*, 2016).

RESULT AND DISCUSSION

Isolation and primary screening of mannanase producing bacteria

Total 13 bacteria were isolated from enriched broth. One bacterial culture was isolated from garden soil sample, 5 were isolated from rhizosphere soil sample, 5 were isolated from compost sample and 2 were isolated from goat dung sample.

Table 6: Zone diameter of mannanase positive bacterial isolates.

Sample	Zone diameter (mm)
R1	12
R2	18
R31	14
R32	11
R4	16
GO1	9
GO2	14
G1	12
C1	19
C2	15
C3	27
C11	24
C4	18

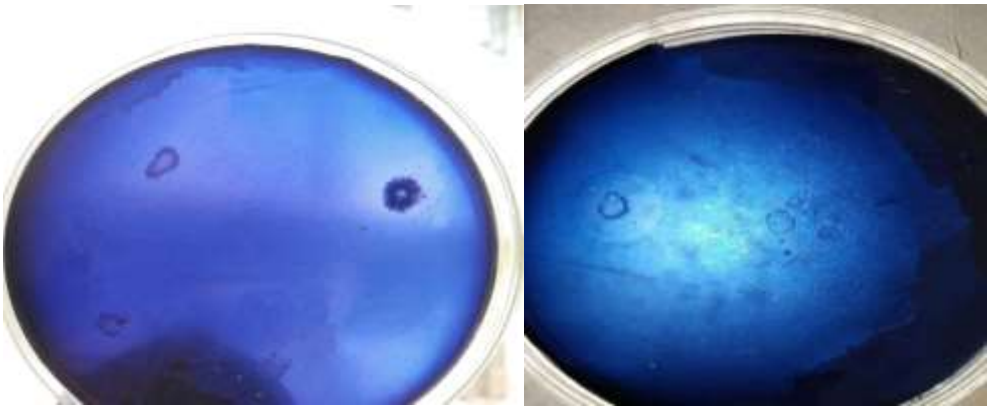

Figure 3: Plate showing clear halo around mannanase positive bacteria.

Table 7: Colony characters of mannanase positive bacterial isolates.

Character	R2	R31	R32	R4	Go1	Go2	G1	C1	C2	C3	C11	C4
Size (mm)	0.2	0.1	0.2	0.4	0.2	0.3	0.2	0.5	0.4	0.3	0.2	0.3
Shape	irregular	circular	circular	Rhizoid	circular	filamentous	circular	irregular	rhizoid	filamentous	circular	punctiform
Pigment	No	No	No	No	No	No	No	Orange	No	No	No	No
Color	White	White	White	White	White	White	White	Orange	Creamy white	Creamy white	white	white
Margin	even	even	Even	filamentous	even	filamentous	even	wavy	filamentous	filamentous	even	even
Elevation	flat	convex	Convex	flat	flat	flat	flat	umbonate	flat	flat	covex	flat
Opacity	translucent	transparent	Opaque	translucent	opaque	translucent	opaque	opaque	translucent	opaque	translucent	transparent
Consistency	dry	sticky	Sticky	sticky	sticky	dry	sticky	sticky	sticky	sticky	sticky	sticky

Secondary Screening of Mannanase producing bacteria

Two bacterial isolates C3 and C11 were showing maximum enzymatic activity 1.073 and 2.061 units, were screened for further studies.

Table 7: Enzyme activity of different mannanase positive bacteria.

Sample	Enzyme Activity (U)
C11	2.061
G2	0.038
R1	0.034
R2	0.043
R42	0.032
C13	0.029
C3	1.073
R32	0.043
C12	0.034
R41	0.039
G1	0.028
Go2	0.029
R31	0.027

Identification of bacterial cultures

Molecular identification of C3 and C11 was done by 16S rRNA gene sequencing. It resulted into following findings.

C3 was identified as *Proteus mirabilis* where as C11 was identified as *Achromobacter denitrificans*.

16S rRNA gene sequence of C3:

ATAGGGGGGGACAGCAGAGCGTGAGAGTGGAGCGGAGGCAGGAGAAAGC
TTGCTTTCTTGCTGACGAGCGGCGCACGGGTGAGTAATGTATGGGGATCTG

CCCGATAGAGGGGGATAACTACTGGAAACGGTGGCTAATACCGCATAATGT
CTACGGACCAAAGCAGGGGCTCTTCGGACCTTGCACTATCGGATGAACCCA
TATGGGATTAGCTAGTAGGTGGGGTAAAGGCTCACCTAGGCGACGATCTCT
AGCTGGTCTGAGAGGATGATCAGCCACACTGGGACTGAGACACGGCCCAG
ACTCCTACGGGAGGCAGCAGTGGGGAATATTGCACAATGGGCGCAAGCCT
GATGCAGCCATGCCGCGTGTATGAAGAAGGCCTTAGGGTTGTAAAGTACTT
TCAGCGGGGAGGAAGGTGATAAGGTTAATACCCTTATCAATTGACGTTACC
CGCAGAAGAAGCACCGGCTAACTCCGTGCCAGCAGCCGCGGTAATACGGA
GGGTGCAAGCGTTAATCGGAATTACTGGGCGTAAAGCGCACGCAGGCGGT
CAATTAAGTCAGATGTGAAAGCCCCGAGCTTAACTTGGGAATTGCATCTGA
AACTGGTTGGCTAGAGTCTTGTAGAGGGGGGTAGAATTCCATGTGTAGCGG
TGAAATGCGTAGAGATGTGGAGGAATACCGGTGGGCGAAGGCGGCCCCCT
GGACAAAGACTGACGCTCAGGTGCGAAAGCGTGGGGAGCAAACAGGATT
AGATACCCTGGTAGTCCACGCTGTAAACGATGTCGATTTAGAGGTTGTGGT
CTTGAACCGTGGCTTCTGGAGCTAACGCGTTAAATCGACCGCCTGGGGAGT
ACGGCCCCAAGGTTAAAACTCAAATGAATTGACGGGGGCCCGCACAAGCG
GTGGAGCATGTGGTTTAATTCGATGCAACGCGAAGAACCTTACCTACTCTT
GACATCCAGCGAATCCTTTAGAGATAGAGGAGTGCCTTCGGGAACGCTGAG
ACAGGTGCTGCATGGCTGTCGTCAGCTCGTGTTGTGAAATGTTGGGTTAAG
TCCCGCAACGAGCGCAACCCTTATCCTTTGTTGCCAGCACGTAATGGTGGG
AACTCAAAGGAGACTGCCGGTGATAAACCGGAGGAAGGTGGGGATGACGT
CAAGTCATCATGGCCCTTACGAGTAGGGCTACACACGTGCTACAATGGCAG
ATACAAAGAGAAGCGACCTCGCGAGAGCAAGCGGAACTCATAAAGTCTGT
CGTAGTCCGGATTGGAGTCTGCAACTCGACTCCATGAAGTCGGAATCGCTA
GTAATCGTAGATCAGAATGCTACGGTGAATACGTTCCCGGGCCTTGTACACA
CCGCCCGTCACACCATGGGAGTGGGTTGCAAAAGAAGTAGGTAGCTTAAC
CTTCGGGAGGGCGCTTACCACTTTGTGATTCATGACTGGGGGTGAAGTCGT
AACAAGGTAAC

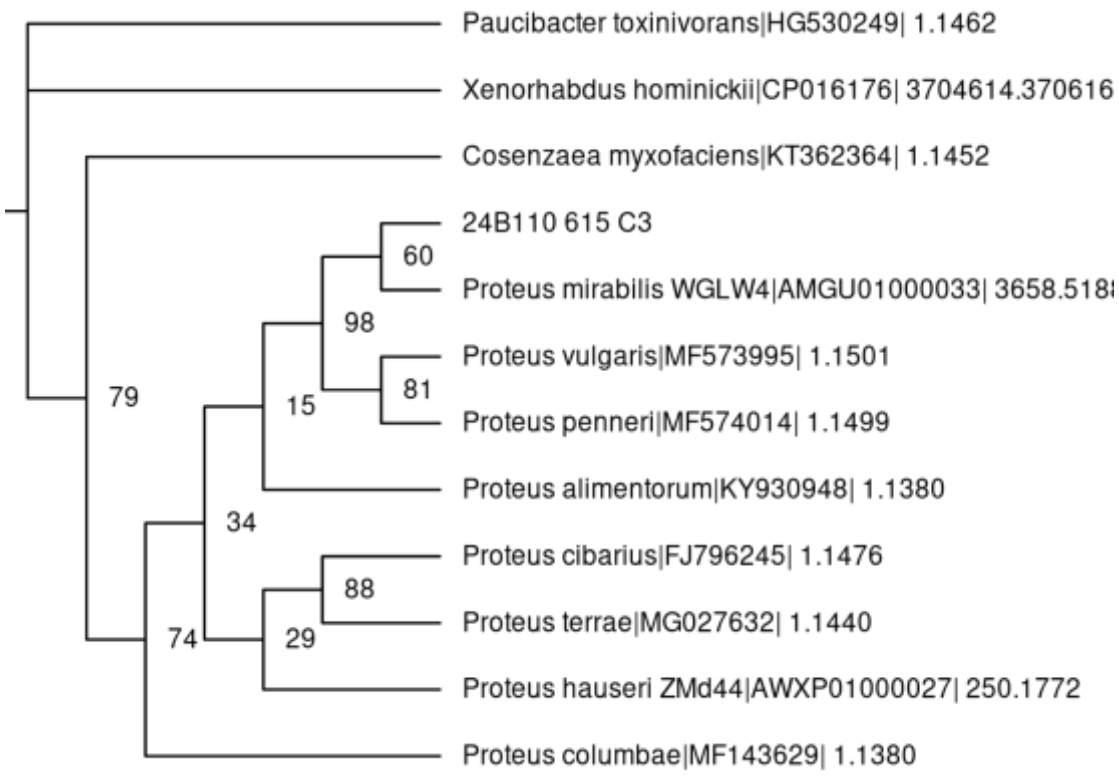

Figure 4: Phylogenetic tree of C3

Table 8: BLAST results of C3

qseqid	Sseqid	pident	length	mismatch	gapopen	qstart	qend	sstart	send	evalue	bitscore
24B110_615_C3	Proteus_mirabilis_WGLW4|AMGU01000033|(3658.5188)	99.449	1453	6	2	26	1478	53	1503	0	2638
24B110_615_C3	Proteus_penneri|MF574014|(1.1499)	99.309	1447	7	3	26	1472	39	1482	0	2614
24B110_615_C3	Proteus_vulgaris|MF573995|(1.1501)	99.107	1455	8	4	26	1477	41	1493	0	2610
24B110_615_C3	Proteus_hauseri_ZMd44|AWXP01000027|(250.1772)	98.761	1453	16	2	26	1478	53	1503	0	2582
24B110_615_C3	Proteus_cibarius|FJ796245|(1.1476)	98.551	1449	17	4	26	1474	32	1476	0	2556
24B110_615_C3	Proteus_terrae|MG027632|(1.1440)	98.403	1440	21	2	26	1465	3	1440	0	2531
24B110_615_C3	Cosenzaea_myxofaciens|KT362364|(1.1452)	98.179	1428	24	2	46	1473	27	1452	0	2492
24B110_615_C3	Proteus_columbae|MF143629|(1.1380)	98.768	1380	16	1	30	1409	2	1380	0	2453
24B110_615_C3	Proteus_alimentorum|KY930948|(1.1380)	98.768	1380	16	1	30	1409	2	1380	0	2453
24B110_615_C3	Xenorhabdus_hominickii|CP016176|(3704614.3706168)	95.891	1436	57	2	43	1478	80	1513	0	2324

16S rRNA gene sequence of C11:

GCACGGGAGCACGGACTTCGGTCTGGTGGCGAGTGGCGAACGGGCGATTA
ATGTATCGGAACGTGCCCAGTAGCGGGGGATAACTACGCGAAAGCGTAGCT
AATACCGCATACGCCCTACGGGGGAAAGCAGGGGATCGCAAGACCTTGCA
CTATTGGAGCGGCCGATATCGGATTAGCTAGTTGGTGGGGTAACGGCTCAC
CAAGGCGACGATCCGTAGCTGGTTTGAGAGGACGACCAGCCACACTGGGA
CTGAGACACGGCCCAGACTCCTACGGGAGGCAGCAGTGGGGAATTTTGGA
CAATGGGGGAAACCCTGATCCAGCCATCCCGCGTGTGCGATGAAGGCCTTC
GGGTTGTAAAGCACTTTTGGCAGGAAAGAAACGTCGTGGGTTAATACCCC
GCGAAACTGACGGTACCTGCAGAATAAGCACCGGCTAACTACGTGCCAGC
AGCCGCGGTAATACGTAGGGTGCAAGCGTTAATCGGAATTACTGGGCGTAA
AGCGTGCGCAGGCGGTTCGGAAAGAAAGATGTGAAATCCCAGAGCTTAAC
TTTGGAACTGCATTTTTAACTACCGGGCTAGAGTGTGTCAGAGGGAGGTGG
AATTCCGCGTGTAGCAGTGAAATGCGTAGATATGCGGAGGAACACCGATGG
CGAAGGCAGCCTCCTGGGATAACACTGACGCTCATGCACGAAAGCGTGGG
GAGCAAACAGGATTAGATACCCTGGTAGTCCACGCCCTAAACGATGTCAAC
TAGCTGTTGGGGCCTTCGGGCCTTGGTAGCGCAGCTAACGCGTGAAGTTGA
CCGCCTGGGGAGTACGGTCGCAAGATTAAAACTCAAAGGAATTGACGGGG
ACCCGCACAAGCGGTGGATGATGTGGATTAATTCGATGCAACGCGAAAAAC
CTTACCTACCCTTGACATGTCTGGAATGCCGAAGAGATTTGGCAGTGCTCG
CAAGAGAACCGGAACACAGGTGCTGCATGGCTGTCGTCAGCTCGTGTCGT
GAGATGTTGGGTTAAGTCCCGCAACGAGCGCAACCCTTGTCATTAGTTGCT
ACGAAAGGGCACTCTAATGAGACTGCCGGTGACAAACCGGAGGAAGGTG
GGGATGACGTCAAGTCCTCATGGCCCTTATGGGTAGGGCTTCACACGTCAT
ACAATGGTCGGGACAGAGGGTCGCCAACCCGCGAGGGGGAGCCAATCCCA
GAAACCCGATCGTAGTCCGGATCGCAGTCTGCAACTCGACTGCGTGAAGTC
GGAATCGCTAGTAATCGCGGATCAGCATGTCGCGGTGAATACGTTCCCGGG
TCTTGTACACACCGCCCGTCACACCATGGGAGTGGGTTTTACCAGAAGTAG
TTAGCCTAACCGCAAGGGGGGCGGATTACCACGGTAGGATTCATGACTGGG
GTGGAAGT

Figure 5: Phylogenetic tree of C11

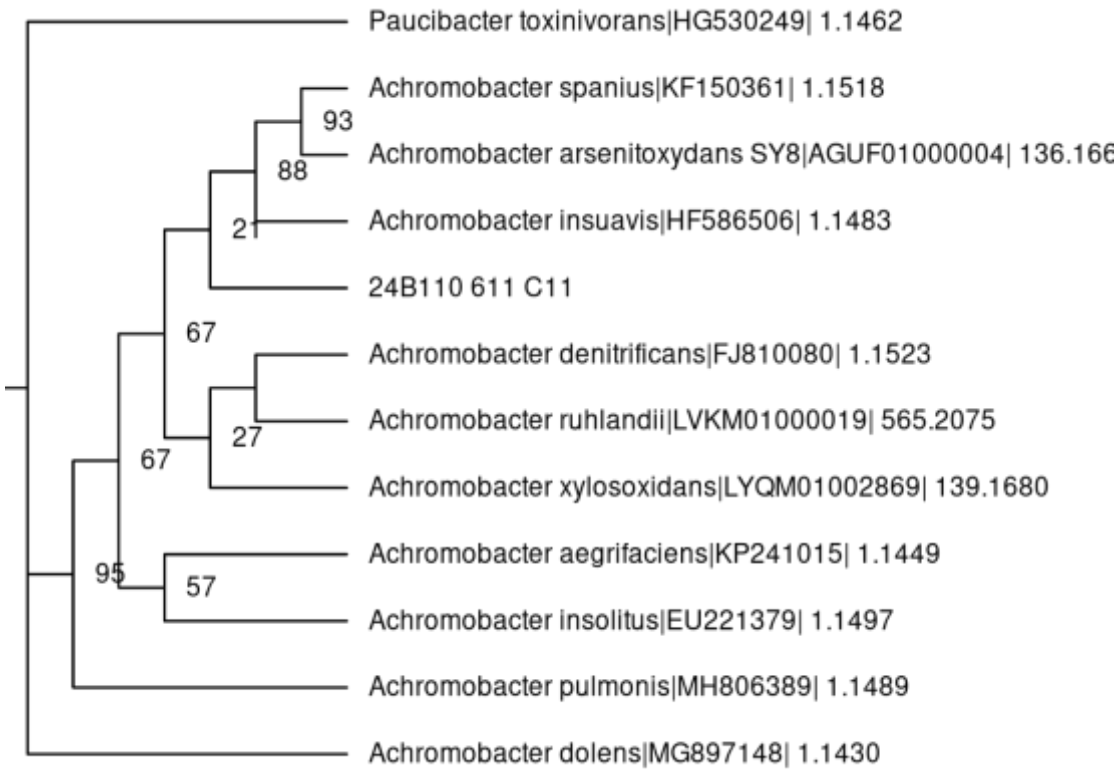

Table 9: BLAST results of C11

Qseqid	Sseqid	pident	length	mismatch	gapopen	qstart	qend	sstart	send	evalue	bitscore
24B110_611_C11	Achromobacter_ruhlandii|LVKM01000019|(565.2075)	99.648	1421	3	2	3	1423	59	1477	0	2595
24B110_611_C11	Achromobacter_xylosoxidans|LYQM01002869|(139.1680)	99.648	1421	3	2	3	1423	73	1491	0	2595
24B110_611_C11	Achromobacter_denitrificans|FJ810080|(1.1523)	99.648	1421	3	2	3	1423	59	1477	0	2595
24B110_611_C11	Achromobacter_insolitus|EU221379|(1.1497)	99.578	1421	4	2	3	1423	62	1480	0	2590
24B110_611_C11	Achromobacter_insuavis|HF586506|(1.1483)	99.507	1421	5	2	3	1423	39	1457	0	2584
24B110_611_C11	Achromobacter_aegrifaciens|KP241015|(1.1449)	99.576	1416	5	1	3	1418	33	1447	0	2580
24B110_611_C11	Achromobacter_arsenitoxydans_SY8|AGUF01000004|(136.1666)	99.296	1421	8	2	3	1423	65	1483	0	2567
24B110_611_C11	Achromobacter_pulmonis|MH806389|(1.1489)	99.296	1421	8	2	3	1423	39	1457	0	2567
24B110_611_C11	Achromobacter_dolens|MG897148|(1.1430)	99.156	1421	10	2	3	1423	9	1427	0	2556
24B110_611_C11	Achromobacter_spanius|KF150361|(1.1518)	99.156	1421	10	2	3	1423	70	1488	0	2556

Optimization of mannanase production from *Proteus mirabilis* and *Achromobacter denitrificans*

Plackett- Burman design results of *Proteus mirabilis*:

Factorial Regression: Absoebance at 540nm versus LBG, Y. E., $(NH4)_2SO_4$, K_2HPO_4, Na_2HPO_4, pH, Temp, Incoculum size (%), PtType

* NOTE * This design has some botched runs.

* NOTE * This design is not orthogonal.

Coded Coefficients

Term	Effect	Coef	SE Coef	T-Value	P-Value	VIF
Constant		0.09500	0.00191	49.67	0.000	
LBG	0.00167	0.00083	0.00191	0.44	0.692	1.02
Y. E.	0.00033	0.00017	0.00191	0.09	0.936	1.02
(NH4)2SO4	0.00667	0.00333	0.00191	1.74	0.180	1.02
K2HPO4	-0.00367	-0.00183	0.00191	-0.96	0.408	1.02
Na2HPO4	0.00033	0.00017	0.00191	0.09	0.936	1.02
pH	0.01367	0.00683	0.00191	3.57	0.037	1.00
Temp	0.00100	0.00050	0.00191	0.26	0.811	1.00
Incoculum size (%)	0.02233	0.01117	0.00191	5.84	0.010	1.02
Ct Pt		0.00798	0.00729	1.09	0.354	1.12

Model Summary

S	R-sq	R-sq(adj)	R-sq(pred)
0.0066249	94.46%	77.82%	*

Analysis of Variance

Source	DF	Adj SS	Adj MS	F-Value	P-Value
Model	9	0.002243	0.000249	5.68	0.090
Linear	8	0.002242	0.000280	6.39	0.077
LBG	1	0.000008	0.000008	0.19	0.692
Y. E.	1	0.000000	0.000000	0.01	0.936
(NH4)2SO4	1	0.000133	0.000133	3.04	0.180
K2HPO4	1	0.000040	0.000040	0.92	0.408
Na2HPO4	1	0.000000	0.000000	0.01	0.936
pH	1	0.000560	0.000560	12.77	0.037
Temp	1	0.000003	0.000003	0.07	0.811
Incoculum size (%)	1	0.001496	0.001496	34.09	0.010
Curvature	1	0.000053	0.000053	1.20	0.354
Error	3	0.000132	0.000044		
Total	12	0.002375			

Regression Equation in Uncoded Units

Absoebance at 540nm = 0.0273 + 0.000125 LBG + 0.00012 Y. E. + 0.00250 (NH4)2SO4 - 0.00137 K2HPO4 + 0.00012 Na2HPO4 + 0.00683 pH + 0.000083 Temp + 0.00836 Incoculum size (%) + 0.00798 Ct Pt

Fits and Diagnostics for Unusual Observations

Obs	Absoebance at 540nm	Fit	Resid	Std Resid	
13	0.09600	0.09600	0.00000		* X

X Unusual X

Alias Structure (up to order 3)

Factor	Name
A	LBG
B	Y. E.
C	(NH4)2SO4
D	K2HPO4
E	Na2HPO4
F	pH
G	Temp
H	Incoculum size (%)

Aliases

I - 0.33 ABC + 0.33 ABD + 0.33 ABE - 0.33 ABF - 0.33 ABG + 0.33 ABH - 0.33 ACD - 0.33 ACE + 0.33 ACF - 0.33 ACG + 0.33 ACH - 0.33 ADE - 0.33 ADF - 0.33 ADG - 0.33 ADH + 0.33 AEF + 0.33 AEG - 0.33 AEH - 0.33 AFG - 0.33 AFH - 0.33 AGH - 0.33 BCD + 0.33 BCE + 0.33 BCF - 0.33 BCG - 0.33 BCH - 0.33 BDE - 0.33 BDF + 0.33 BDG - 0.33 BDH - 0.33 BEF - 0.33 BEG - 0.33 BEH + 0.33 BFG + 0.33 BFH - 0.33 BGH - 0.33 CDE + 0.33 CDF + 0.33 CDG - 0.33 CDH - 0.33 CEF - 0.33 CEG + 0.33 CEH - 0.33 CFG + 0.33 CFH + 0.33 CGH - 0.33 DEF + 0.33 DEG + 0.33 DEH - 0.33 DFG - 0.33 DFH - 0.33 DGH - 0.33 EFG + 0.33 EFH - 0.33 EGH - 0.33 FGH

A - 0.33 BC + 0.33 BD + 0.33 BE - 0.33 BF - 0.33 BG + 0.33 BH - 0.33 CD - 0.33 CE + 0.33 CF - 0.33 CG + 0.33 CH - 0.33 DE - 0.33 DF - 0.33 DG - 0.33 DH + 0.33 EF + 0.33 EG - 0.33 EH - 0.33 FG - 0.33 FH - 0.33 GH - 0.33 BCD + 0.33 BCE + 0.33 BCF + 0.33 BCG + 0.33 BCH + 0.33 BDE - 0.33 BDF + 0.33 BDG + 0.33 BDH + 0.33 BEF + 0.33 BEG + 0.33 BEH - 0.33 BFG + 0.33 BFH - 0.33 BGH + 0.33 CDE + 0.33 CDF - 0.33 CDG - 0.33 CDH + 0.33 CEF - 0.33 CEG + 0.33 CEH - 0.33 CFG + 0.33 CFH + 0.33 CGH - 0.33 DEF + 0.33 DEG - 0.33 DEH + 0.33 DFG + 0.33 DFH + 0.33 DGH + 0.33 EFG + 0.33 EFH - 0.33 EGH + 0.33 FGH

B - 0.33 AC + 0.33 AD + 0.33 AE - 0.33 AF - 0.33 AG + 0.33 AH - 0.33 CD + 0.33 CE + 0.33 CF - 0.33 CG - 0.33 CH - 0.33 DE - 0.33 DF + 0.33 DG - 0.33 DH - 0.33 EF - 0.33 EG - 0.33 EH + 0.33 FG + 0.33 FH - 0.33 GH - 0.33 ACD + 0.33 ACE + 0.33 ACF + 0.33 ACG + 0.33 ACH + 0.33 ADE - 0.33 ADF + 0.33 ADG + 0.33 ADH + 0.33 AEF + 0.33 AEG + 0.33 AEH - 0.33 AFG + 0.33 AFH - 0.33 AGH - 0.33 CDE + 0.33 CDF + 0.33 CDG + 0.33 CDH + 0.33 CEF - 0.33 CEG + 0.33 CEH + 0.33 CFG + 0.33 CFH - 0.33 CGH + 0.33 DEF + 0.33 DEG - 0.33 DEH + 0.33 DFG - 0.33 DFH - 0.33 DGH - 0.33 EFG + 0.33 EFH + 0.33 EGH + 0.33 FGH

C - 0.33 AB - 0.33 AD - 0.33 AE + 0.33 AF - 0.33 AG + 0.33 AH - 0.33 BD + 0.33 BE + 0.33 BF - 0.33 BG - 0.33 BH - 0.33 DE + 0.33 DF + 0.33 DG - 0.33 DH - 0.33 EF - 0.33 EG + 0.33 EH - 0.33 FG - 0.33 FH + 0.33 GH - 0.33 ABD + 0.33 ABE + 0.33 ABF + 0.33 ABG + 0.33 ABH + 0.33 ADE + 0.33 ADF - 0.33 ADG - 0.33 ADH + 0.33 AEF - 0.33 AEG + 0.33 AEH - 0.33 AFG + 0.33 AFH + 0.33 AGH - 0.33 BDE + 0.33 BDF + 0.33 BDG + 0.33 BDH + 0.33 BEF - 0.33 BEG + 0.33 BEH + 0.33 BFG + 0.33 BFH - 0.33 BGH - 0.33 DEF + 0.33 DEG + 0.33 DEH + 0.33 DFG - 0.33 DFH + 0.33 DGH + 0.33 EFG + 0.33 EFH + 0.33 EGH - 0.33 FGH

D + 0.33 AB - 0.33 AC - 0.33 AE - 0.33 AF - 0.33 AG - 0.33 AH - 0.33 BC - 0.33 BE - 0.33 BF + 0.33 BG - 0.33 BH - 0.33 CE + 0.33 CF + 0.33 CG - 0.33 CH - 0.33 EF + 0.33 EG + 0.33 EH - 0.33 FG - 0.33 FH - 0.33 GH - 0.33 ABC + 0.33 ABE - 0.33 ABF + 0.33 ABG + 0.33 ABH + 0.33 ACE + 0.33 ACF - 0.33 ACG - 0.33 ACH - 0.33 AEF + 0.33 AEG - 0.33 AEH + 0.33 AFG + 0.33 AFH + 0.33 AGH - 0.33 BCE + 0.33 BCF + 0.33 BCG + 0.33 BCH + 0.33 BEF + 0.33 BEG - 0.33 BEH + 0.33 BFG - 0.33 BFH - 0.33 BGH - 0.33 CEF + 0.33 CEG + 0.33 CEH + 0.33 CFG - 0.33 CFH + 0.33 CGH - 0.33 EFG + 0.33 EFH + 0.33 EGH + 0.33 FGH

E + 0.33 AB - 0.33 AC - 0.33 AD + 0.33 AF + 0.33 AG - 0.33 AH + 0.33 BC - 0.33 BD - 0.33 BF - 0.33 BG - 0.33 BH - 0.33 CD - 0.33 CF - 0.33 CG + 0.33 CH - 0.33 DF + 0.33 DG + 0.33 DH - 0.33 FG + 0.33 FH - 0.33 GH + 0.33 ABC + 0.33 ABD + 0.33 ABF + 0.33 ABG + 0.33 ABH + 0.33 ACD + 0.33 ACF - 0.33 ACG + 0.33 ACH - 0.33 ADF + 0.33 ADG - 0.33 ADH + 0.33 AFG + 0.33 AFH - 0.33 AGH - 0.33 BCD + 0.33 BCF - 0.33 BCG + 0.33 BCH + 0.33 BDF + 0.33 BDG - 0.33 BDH - 0.33 BFG + 0.33 BFH + 0.33 BGH - 0.33 CDF + 0.33 CDG + 0.33 CDH + 0.33 CFG + 0.33 CFH + 0.33 CGH - 0.33 DFG + 0.33 DFH + 0.33 DGH - 0.33 FGH

F - 0.33 AB + 0.33 AC - 0.33 AD + 0.33 AE - 0.33 AG - 0.33 AH + 0.33 BC - 0.33 BD - 0.33 BE
+ 0.33 BG + 0.33 BH + 0.33 CD - 0.33 CE - 0.33 CG - 0.33 CH - 0.33 DE - 0.33 DG - 0.33 DH
- 0.33 EG + 0.33 EH - 0.33 GH + 0.33 ABC - 0.33 ABD + 0.33 ABE - 0.33 ABG + 0.33 ABH
+ 0.33 ACD + 0.33 ACE - 0.33 ACG + 0.33 ACH - 0.33 ADE + 0.33 ADG + 0.33 ADH + 0.33 AEG
+ 0.33 AEH + 0.33 AGH + 0.33 BCD + 0.33 BCE + 0.33 BCG + 0.33 BCH + 0.33 BDE + 0.33 BDG
- 0.33 BDH - 0.33 BEG + 0.33 BEH + 0.33 BGH - 0.33 CDE + 0.33 CDG - 0.33 CDH + 0.33 CEG
+ 0.33 CEH - 0.33 CGH - 0.33 DEG + 0.33 DEH + 0.33 DGH - 0.33 EGH

G - 0.33 AB - 0.33 AC - 0.33 AD + 0.33 AE - 0.33 AF - 0.33 AH - 0.33 BC + 0.33 BD - 0.33 BE
+ 0.33 BF - 0.33 BH + 0.33 CD - 0.33 CE - 0.33 CF + 0.33 CH + 0.33 DE - 0.33 DF - 0.33 DH
- 0.33 EF - 0.33 EH - 0.33 FH + 0.33 ABC + 0.33 ABD + 0.33 ABE - 0.33 ABF - 0.33 ABH
- 0.33 ACD - 0.33 ACE - 0.33 ACF + 0.33 ACH + 0.33 ADE + 0.33 ADF + 0.33 ADH + 0.33 AEF
- 0.33 AEH + 0.33 AFH + 0.33 BCD - 0.33 BCE + 0.33 BCF - 0.33 BCH + 0.33 BDE + 0.33 BDF
- 0.33 BDH - 0.33 BEF + 0.33 BEH + 0.33 BFH + 0.33 CDE + 0.33 CDF + 0.33 CDH + 0.33 CEF
+ 0.33 CEH - 0.33 CFH - 0.33 DEF + 0.33 DEH + 0.33 DFH - 0.33 EFH

H + 0.33 AB + 0.33 AC - 0.33 AD - 0.33 AE - 0.33 AF - 0.33 AG - 0.33 BC - 0.33 BD - 0.33 BE
+ 0.33 BF - 0.33 BG - 0.33 CD + 0.33 CE - 0.33 CF + 0.33 CG + 0.33 DE - 0.33 DF - 0.33 DG
+ 0.33 EF - 0.33 EG - 0.33 FG + 0.33 ABC + 0.33 ABD + 0.33 ABE + 0.33 ABF - 0.33 ABG
- 0.33 ACD + 0.33 ACE + 0.33 ACF + 0.33 ACG - 0.33 ADE + 0.33 ADF + 0.33 ADG + 0.33 AEF
- 0.33 AEG + 0.33 AFG + 0.33 BCD + 0.33 BCE + 0.33 BCF - 0.33 BCG - 0.33 BDE - 0.33 BDF
- 0.33 BDG + 0.33 BEF + 0.33 BEG + 0.33 BFG + 0.33 CDE - 0.33 CDF + 0.33 CDG + 0.33 CEF
+ 0.33 CEG - 0.33 CFG + 0.33 DEF + 0.33 DEG + 0.33 DFG - 0.33 EFG

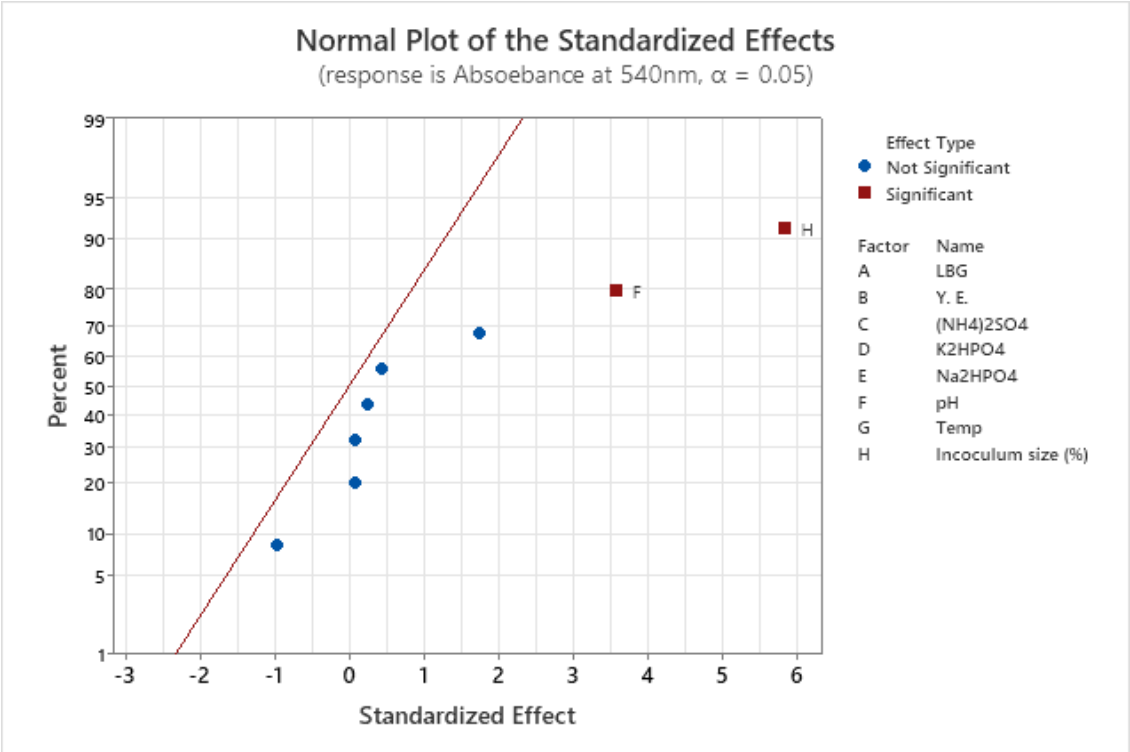

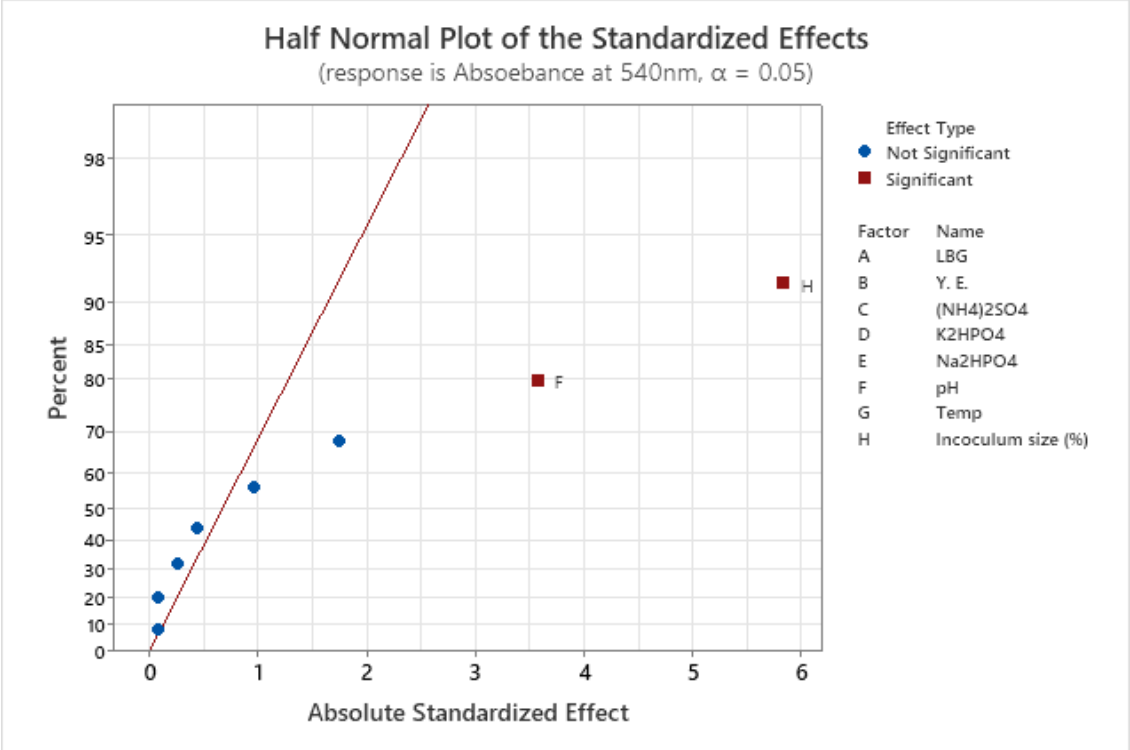
Half Normal Plot of the Standardized Effects
(response is Absoebance at 540nm, α = 0.05)
Percent
98
95
90
85
80
70
60
50
40
30
20
10
0
H
F
0
1
2
3
4
5
6
Absolute Standardized Effect
Effect Type
Not Significant
Significant
Factor Name
A LBG
B Y. E.
C (NH4)2SO4
D K2HPO4
E Na2HPO4
F pH
G Temp
H Incoculum size (%)

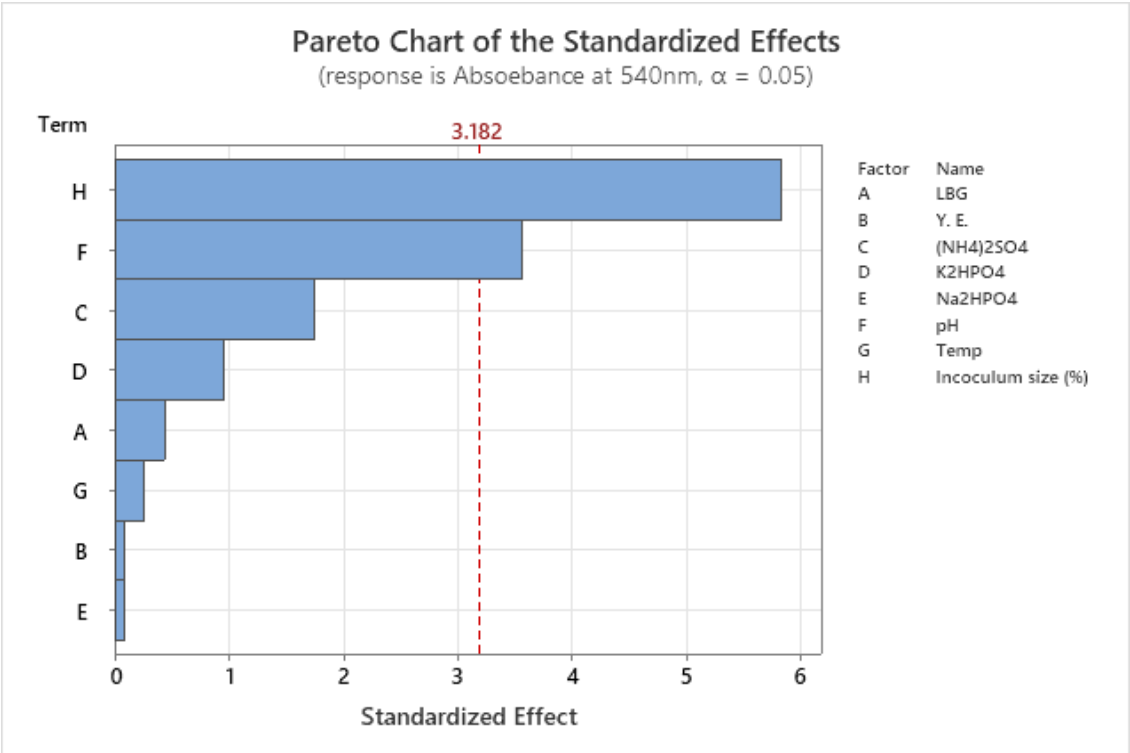
Pareto Chart of the Standardized Effects
(response is Absoebance at 540nm, α = 0.05)
Term
3.182
H
F
C
D
A
G
B
E
0
1
2
3
4
5
6
Standardized Effect
Factor Name
A LBG
B Y. E.
C (NH4)2SO4
D K2HPO4
E Na2HPO4
F pH
G Temp
H Incoculum size (%)

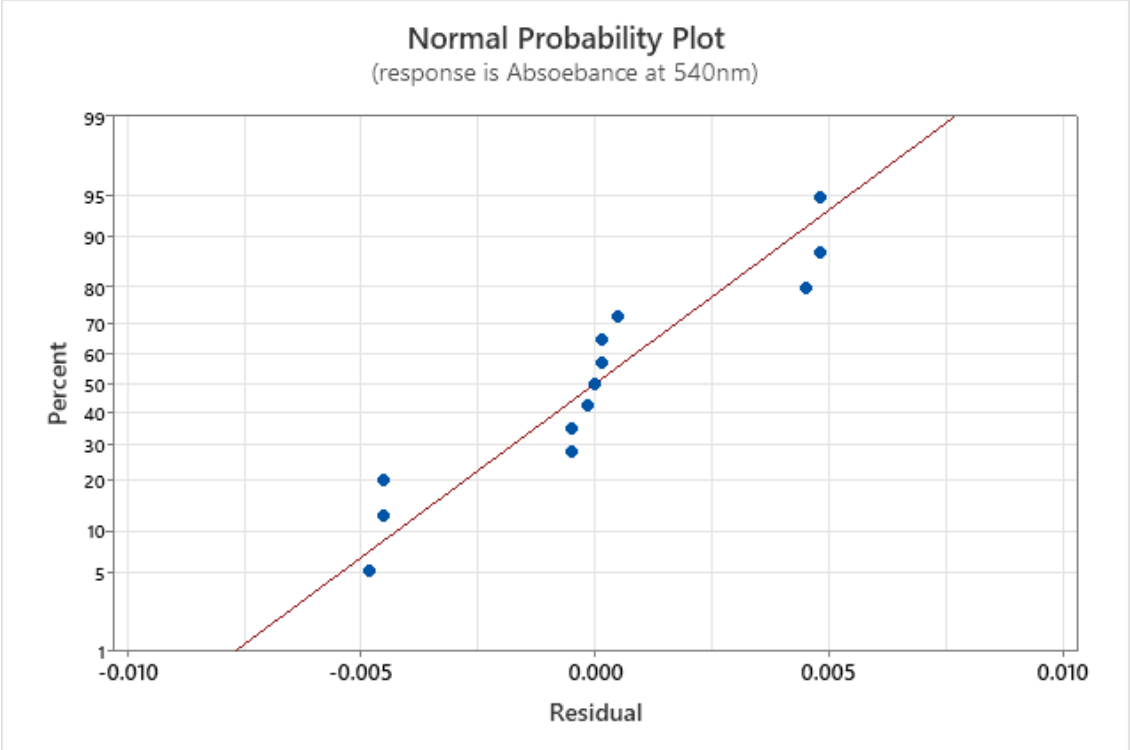
Normal Probability Plot
(response is Absoebance at 540nm)
Percent
99
95
90
80
70
60
50
40
30
20
10
5
1
-0.010
-0.005
0.000
0.005
0.010
Residual

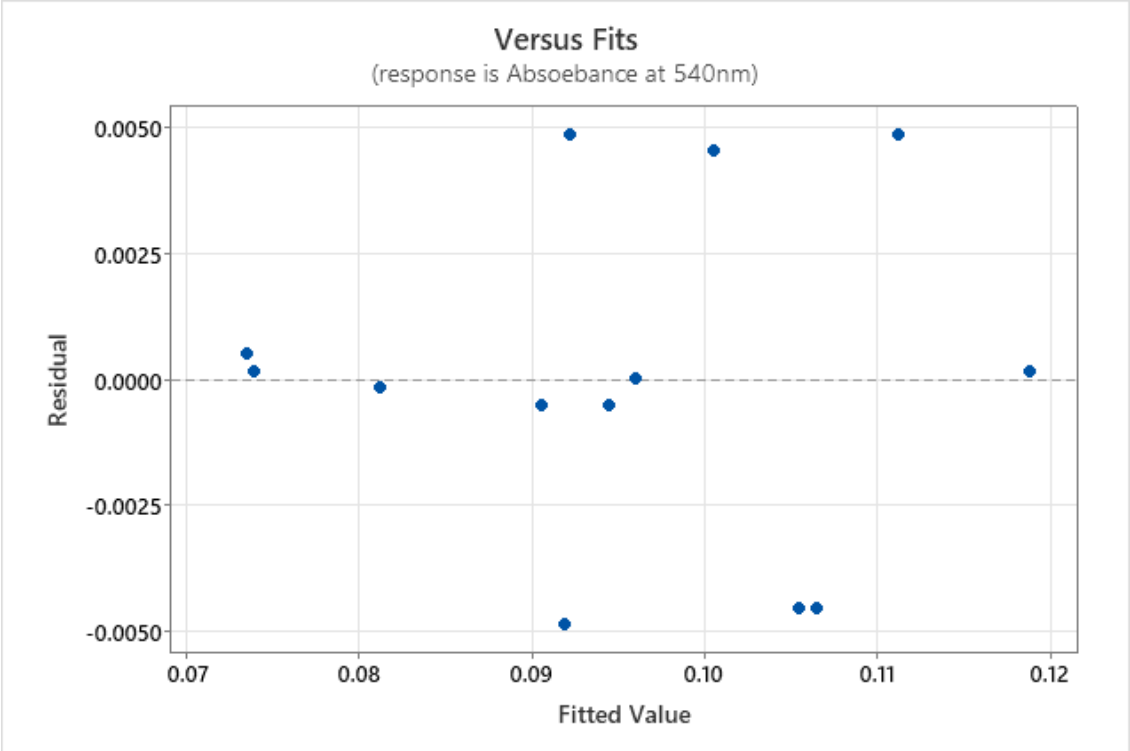
Versus Fits
(response is Absoebance at 540nm)
Residual
0.0050
0.0025
0.0000
-0.0025
-0.0050
0.07
0.08
0.09
0.10
0.11
0.12
Fitted Value

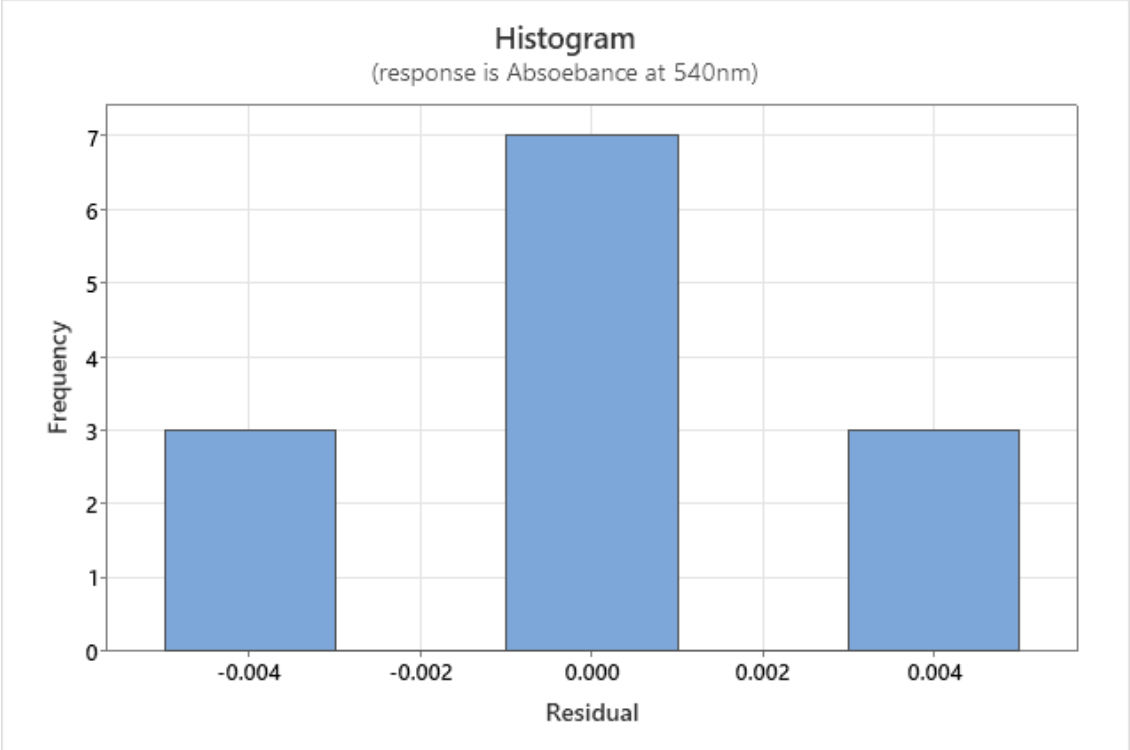
Histogram
(response is Absoebance at 540nm)
Frequency
0
1
2
3
4
5
6
7
-0.004
-0.002
0.000
0.002
0.004
Residual

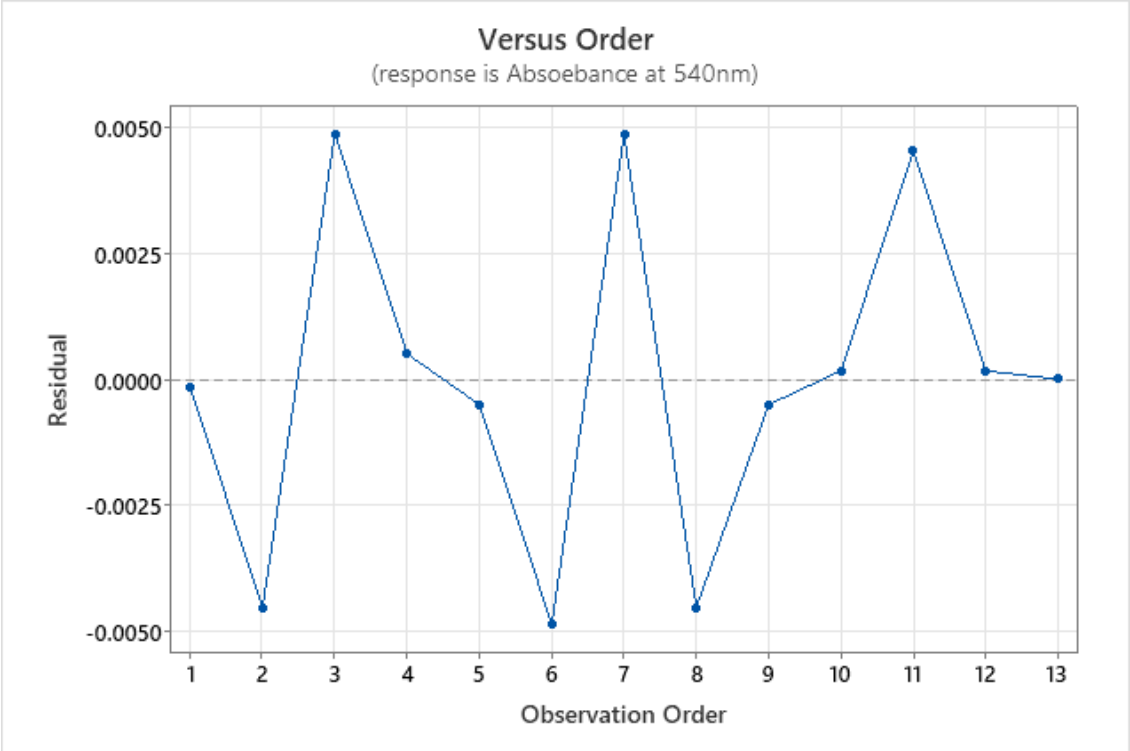
Versus Order
(response is Absoebance at 540nm)
Residual
0.0050
0.0025
0.0000
-0.0025
-0.0050
1
2
3
4
5
6
7
8
9
10
11
12
13
Observation Order

Plackett- Burman design results of *Achromobacter denitrificans*:

Factorial Regression: Absorbance at 540nm versus LBG, Y. E., (NH4)2SO4, K2HPO4, Na2HPO4, pH, Temp, Incoculum size (%), PtType

* NOTE * This design has some botched runs.

* NOTE * This design is not orthogonal.

Coded Coefficients

Term	Effect	Coef	SE Coef	T-Value	P-Value	VIF
Constant		0.06117	0.00245	24.93	0.000	
LBG	0.01967	0.00983	0.00245	4.01	0.028	1.02
Y. E.	-0.00467	-0.00233	0.00245	-0.95	0.412	1.02
(NH4)2SO4	0.01200	0.00600	0.00245	2.45	0.092	1.02
K2HPO4	-0.00667	-0.00333	0.00245	-1.36	0.267	1.02
Na2HPO4	0.00633	0.00317	0.00245	1.29	0.287	1.02
pH	0.01667	0.00833	0.00245	3.40	0.043	1.00
Temp	-0.00533	-0.00267	0.00245	-1.09	0.357	1.00
Incoculum size (%)	-0.01100	-0.00550	0.00245	-2.24	0.111	1.02
Ct Pt		0.03131	0.00935	3.35	0.044	1.12

Model Summary

S	R-sq	R-sq(adj)	R-sq(pred)
0.0084984	94.75%	78.99%	*

Analysis of Variance

Source	DF	Adj SS	Adj MS	F-Value	P-Value
Model	9	0.003908	0.000434	6.01	0.084
Linear	8	0.003193	0.000399	5.53	0.094
LBG	1	0.001160	0.001160	16.07	0.028
Y. E.	1	0.000065	0.000065	0.90	0.412
(NH4)2SO4	1	0.000432	0.000432	5.98	0.092
K2HPO4	1	0.000133	0.000133	1.85	0.267
Na2HPO4	1	0.000120	0.000120	1.67	0.287
pH	1	0.000833	0.000833	11.54	0.043
Temp	1	0.000085	0.000085	1.18	0.357
Incoculum size (%)	1	0.000363	0.000363	5.03	0.111
Curvature	1	0.000810	0.000810	11.22	0.044
Error	3	0.000217	0.000072		
Total	12	0.004125			

Regression Equation in Uncoded Units

Absorbance at 540nm = 0.0068 + 0.001475 LBG - 0.00175 Y. E. + 0.00449 (NH4)2SO4 - 0.00250 K2HPO4 + 0.00237 Na2HPO4 + 0.00833 pH - 0.000444 Temp - 0.00412 Incoculum size (%) + 0.03131 Ct Pt

Fits and Diagnostics for Unusual Observations

Obs	Absorbance at 540nm	Fit	Resid	Std Resid	
13	0.08900	0.08900	0.00000	*	X

X Unusual X

Alias Structure (up to order 3)

Factor	Name
A	LBG
B	Y. E.
C	(NH4)2SO4
D	K2HPO4
E	Na2HPO4
F	pH
G	Temp
H	Incoculum size (%)

Aliases

I - 0.33 ABC + 0.33 ABD + 0.33 ABE - 0.33 ABF - 0.33 ABG + 0.33 ABH - 0.33 ACD - 0.33 ACE
+ 0.33 ACF - 0.33 ACG + 0.33 ACH - 0.33 ADE - 0.33 ADF - 0.33 ADG - 0.33 ADH + 0.33 AEF
+ 0.33 AEG - 0.33 AEH - 0.33 AFG - 0.33 AFH - 0.33 AGH - 0.33 BCD + 0.33 BCE + 0.33 BCF
- 0.33 BCG - 0.33 BCH - 0.33 BDE - 0.33 BDF + 0.33 BDG - 0.33 BDH - 0.33 BEF - 0.33 BEG
- 0.33 BEH + 0.33 BFG + 0.33 BFH - 0.33 BGH - 0.33 CDE + 0.33 CDF + 0.33 CDG - 0.33 CDH
- 0.33 CEF - 0.33 CEG + 0.33 CEH - 0.33 CFG - 0.33 CFH + 0.33 CGH - 0.33 DEF + 0.33 DEG
+ 0.33 DEH - 0.33 DFG - 0.33 DFH - 0.33 DGH - 0.33 EFG + 0.33 EFH - 0.33 EGH - 0.33 FGH

A - 0.33 BC + 0.33 BD + 0.33 BE - 0.33 BF - 0.33 BG + 0.33 BH - 0.33 CD - 0.33 CE + 0.33 CF
- 0.33 CG + 0.33 CH - 0.33 DE - 0.33 DF - 0.33 DG - 0.33 DH + 0.33 EF + 0.33 EG - 0.33 EH
- 0.33 FG - 0.33 FH - 0.33 GH - 0.33 BCD + 0.33 BCE + 0.33 BCF + 0.33 BCG + 0.33 BCH
+ 0.33 BDE - 0.33 BDF + 0.33 BDG + 0.33 BDH + 0.33 BEF + 0.33 BEG + 0.33 BEH - 0.33 BFG
+ 0.33 BFH - 0.33 BGH + 0.33 CDE + 0.33 CDF - 0.33 CDG - 0.33 CDH + 0.33 CEF - 0.33 CEG
+ 0.33 CEH - 0.33 CFG + 0.33 CFH + 0.33 CGH - 0.33 DEF + 0.33 DEG - 0.33 DEH + 0.33 DFG
+ 0.33 DFH + 0.33 DGH + 0.33 EFG + 0.33 EFH - 0.33 EGH + 0.33 FGH

B - 0.33 AC + 0.33 AD + 0.33 AE - 0.33 AF - 0.33 AG + 0.33 AH - 0.33 CD + 0.33 CE + 0.33 CF
- 0.33 CG - 0.33 CH - 0.33 DE - 0.33 DF + 0.33 DG - 0.33 DH - 0.33 EF - 0.33 EG - 0.33 EH
+ 0.33 FG + 0.33 FH - 0.33 GH - 0.33 ACD + 0.33 ACE + 0.33 ACF + 0.33 ACG + 0.33 ACH
+ 0.33 ADE - 0.33 ADF + 0.33 ADG + 0.33 ADH + 0.33 AEF + 0.33 AEG + 0.33 AEH - 0.33 AFG
+ 0.33 AFH - 0.33 AGH - 0.33 CDE + 0.33 CDF + 0.33 CDG + 0.33 CDH + 0.33 CEF - 0.33 CEG
+ 0.33 CEH + 0.33 CFG + 0.33 CFH - 0.33 CGH + 0.33 DEF + 0.33 DEG - 0.33 DEH + 0.33 DFG
- 0.33 DFH - 0.33 DGH - 0.33 EFG + 0.33 EFH + 0.33 EGH + 0.33 FGH

C - 0.33 AB - 0.33 AD - 0.33 AE + 0.33 AF - 0.33 AG + 0.33 AH - 0.33 BD + 0.33 BE + 0.33 BF
- 0.33 BG - 0.33 BH - 0.33 DE + 0.33 DF + 0.33 DG - 0.33 DH - 0.33 EF - 0.33 EG + 0.33 EH
- 0.33 FG - 0.33 FH + 0.33 GH - 0.33 ABD + 0.33 ABE + 0.33 ABF + 0.33 ABG + 0.33 ABH
+ 0.33 ADE + 0.33 ADF - 0.33 ADG - 0.33 ADH + 0.33 AEF - 0.33 AEG + 0.33 AEH - 0.33 AFG
+ 0.33 AFH + 0.33 AGH - 0.33 BDE + 0.33 BDF + 0.33 BDG + 0.33 BDH + 0.33 BEF - 0.33 BEG
+ 0.33 BEH + 0.33 BFG + 0.33 BFH - 0.33 BGH - 0.33 DEF + 0.33 DEG + 0.33 DEH + 0.33 DFG
- 0.33 DFH + 0.33 DGH + 0.33 EFG + 0.33 EFH + 0.33 EGH - 0.33 FGH

D + 0.33 AB - 0.33 AC - 0.33 AE - 0.33 AF - 0.33 AG - 0.33 AH - 0.33 BC - 0.33 BE - 0.33 BF
+ 0.33 BG - 0.33 BH - 0.33 CE + 0.33 CF + 0.33 CG - 0.33 CH - 0.33 EF + 0.33 EG + 0.33 EH
- 0.33 FG - 0.33 FH - 0.33 GH - 0.33 ABC + 0.33 ABE - 0.33 ABF + 0.33 ABG + 0.33 ABH
+ 0.33 ACE + 0.33 ACF - 0.33 ACG - 0.33 ACH - 0.33 AEF + 0.33 AEG - 0.33 AEH + 0.33 AFG
+ 0.33 AFH + 0.33 AGH - 0.33 BCE + 0.33 BCF + 0.33 BCG + 0.33 BCH + 0.33 BEF + 0.33 BEG
- 0.33 BEH + 0.33 BFG - 0.33 BFH - 0.33 BGH - 0.33 CEF + 0.33 CEG + 0.33 CEH + 0.33 CFG
- 0.33 CFH + 0.33 CGH - 0.33 EFG + 0.33 EFH + 0.33 EGH + 0.33 FGH

E + 0.33 AB - 0.33 AC - 0.33 AD + 0.33 AF + 0.33 AG - 0.33 AH + 0.33 BC - 0.33 BD - 0.33 BF
- 0.33 BG - 0.33 BH - 0.33 CD - 0.33 CF - 0.33 CG + 0.33 CH - 0.33 DF + 0.33 DG + 0.33 DH
- 0.33 FG + 0.33 FH - 0.33 GH + 0.33 ABC + 0.33 ABD + 0.33 ABF + 0.33 ABG + 0.33 ABH
+ 0.33 ACD + 0.33 ACF - 0.33 ACG + 0.33 ACH - 0.33 ADF + 0.33 ADG - 0.33 ADH + 0.33 AFG
+ 0.33 AFH - 0.33 AGH - 0.33 BCD + 0.33 BCF - 0.33 BCG + 0.33 BCH + 0.33 BDF + 0.33 BDG
- 0.33 BDH - 0.33 BFG + 0.33 BFH + 0.33 BGH - 0.33 CDF + 0.33 CDG + 0.33 CDH + 0.33 CFG
+ 0.33 CFH + 0.33 CGH - 0.33 DFG + 0.33 DFH + 0.33 DGH - 0.33 FGH

F - 0.33 AB + 0.33 AC - 0.33 AD + 0.33 AE - 0.33 AG - 0.33 AH + 0.33 BC - 0.33 BD - 0.33 BE
+ 0.33 BG + 0.33 BH + 0.33 CD - 0.33 CE - 0.33 CG - 0.33 CH - 0.33 DE - 0.33 DG - 0.33 DH
- 0.33 EG + 0.33 EH - 0.33 GH + 0.33 ABC - 0.33 ABD + 0.33 ABE - 0.33 ABG + 0.33 ABH
+ 0.33 ACD + 0.33 ACE - 0.33 ACG + 0.33 ACH - 0.33 ADE + 0.33 ADG + 0.33 ADH + 0.33 AEG
+ 0.33 AEH + 0.33 AGH + 0.33 BCD + 0.33 BCE + 0.33 BCG + 0.33 BCH + 0.33 BDE + 0.33 BDG
- 0.33 BDH - 0.33 BEG + 0.33 BEH + 0.33 BGH - 0.33 CDE + 0.33 CDG - 0.33 CDH + 0.33 CEG
+ 0.33 CEH - 0.33 CGH - 0.33 DEG + 0.33 DEH + 0.33 DGH - 0.33 EGH

G - 0.33 AB - 0.33 AC - 0.33 AD + 0.33 AE - 0.33 AF - 0.33 AH - 0.33 BC + 0.33 BD - 0.33 BE
+ 0.33 BF - 0.33 BH + 0.33 CD - 0.33 CE - 0.33 CF + 0.33 CH + 0.33 DE - 0.33 DF - 0.33 DH
- 0.33 EF - 0.33 EH - 0.33 FH + 0.33 ABC + 0.33 ABD + 0.33 ABE - 0.33 ABF - 0.33 ABH
- 0.33 ACD - 0.33 ACE - 0.33 ACF + 0.33 ACH + 0.33 ADE + 0.33 ADF + 0.33 ADH + 0.33 AEF
- 0.33 AEH + 0.33 AFH + 0.33 BCD - 0.33 BCE + 0.33 BCF - 0.33 BCH + 0.33 BDE + 0.33 BDF
- 0.33 BDH - 0.33 BEF + 0.33 BEH + 0.33 BFH + 0.33 CDE + 0.33 CDF + 0.33 CDH + 0.33 CEF
+ 0.33 CEH - 0.33 CFH - 0.33 DEF + 0.33 DEH + 0.33 DFH - 0.33 EFH

H + 0.33 AB + 0.33 AC - 0.33 AD - 0.33 AE - 0.33 AF - 0.33 AG - 0.33 BC - 0.33 BD - 0.33 BE
+ 0.33 BF - 0.33 BG - 0.33 CD + 0.33 CE - 0.33 CF + 0.33 CG + 0.33 DE - 0.33 DF - 0.33 DG
+ 0.33 EF - 0.33 EG - 0.33 FG + 0.33 ABC + 0.33 ABD + 0.33 ABE + 0.33 ABF - 0.33 ABG

- 0.33 ACD + 0.33 ACE + 0.33 ACF + 0.33 ACG - 0.33 ADE + 0.33 ADF + 0.33 ADG + 0.33 AEF
- 0.33 AEG + 0.33 AFG + 0.33 BCD + 0.33 BCE + 0.33 BCF - 0.33 BCG - 0.33 BDE - 0.33 BDF
- 0.33 BDG + 0.33 BEF + 0.33 BEG + 0.33 BFG + 0.33 CDE - 0.33 CDF + 0.33 CDG + 0.33 CEF
+ 0.33 CEG - 0.33 CFG + 0.33 DEF + 0.33 DEG + 0.33 DFG - 0.33 EFG

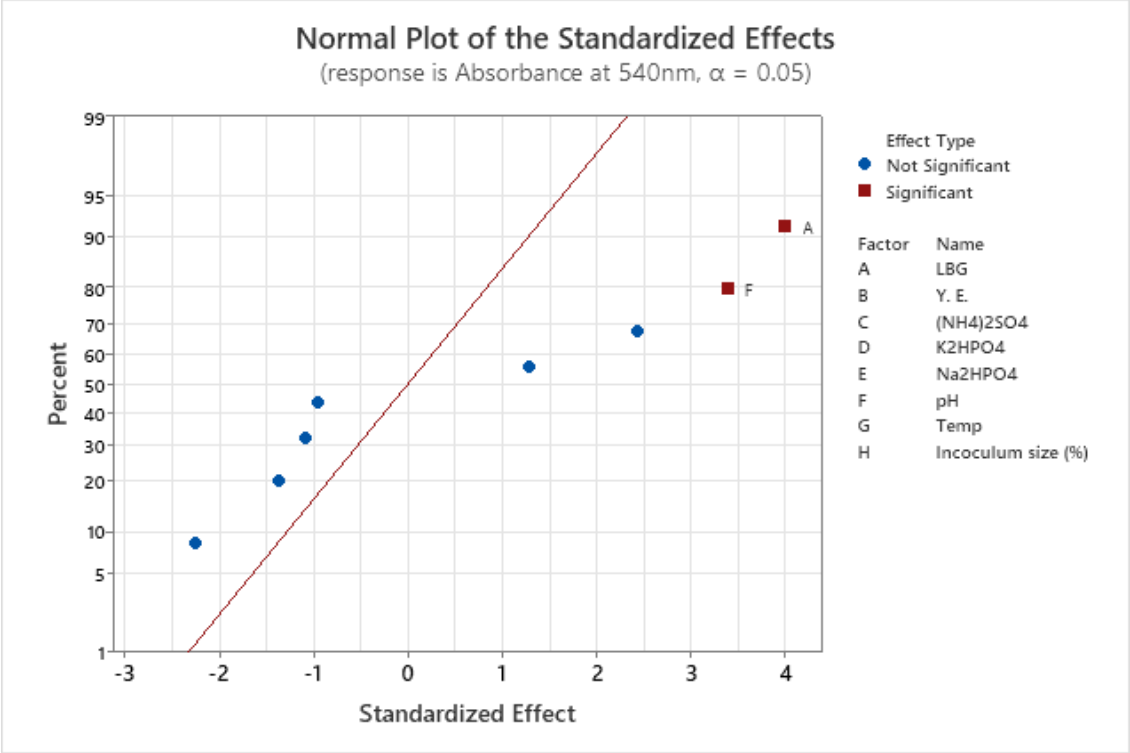

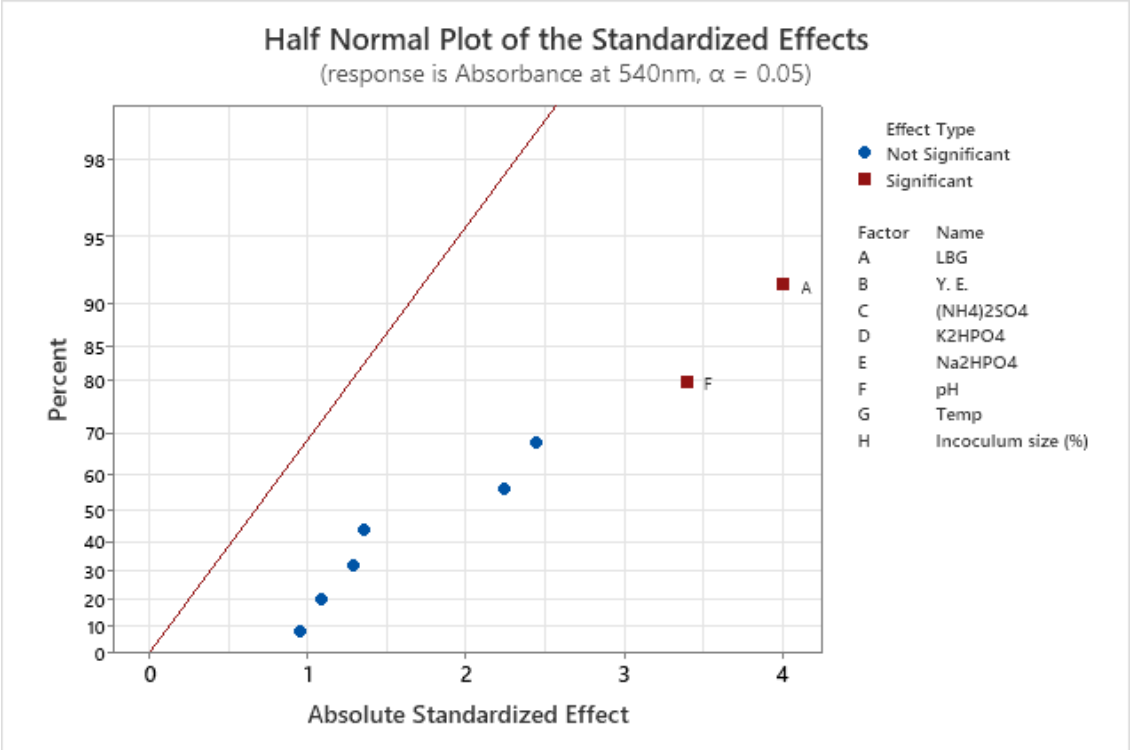

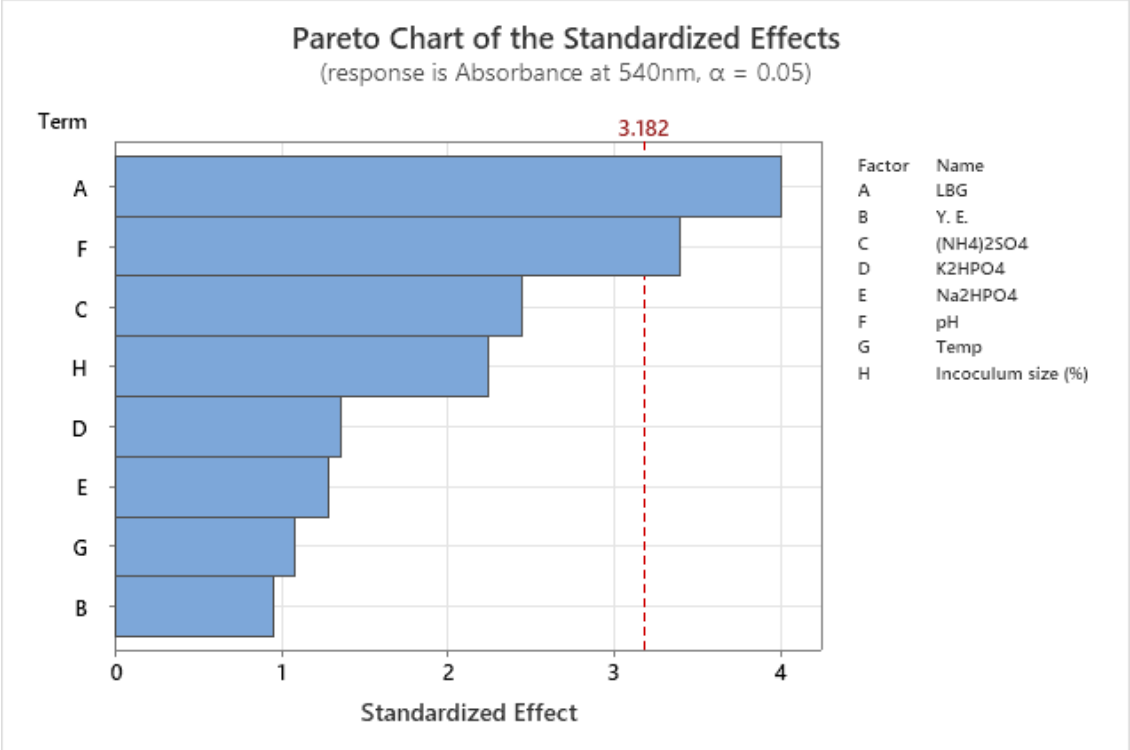
Pareto Chart of the Standardized Effects
(response is Absorbance at 540nm, α = 0.05)
Term
3.182
A
F
C
H
D
E
G
B
0
1
2
3
4
Standardized Effect
Factor Name
A LBG
B Y. E.
C (NH4)2SO4
D K2HPO4
E Na2HPO4
F pH
G Temp
H Incoculum size (%)

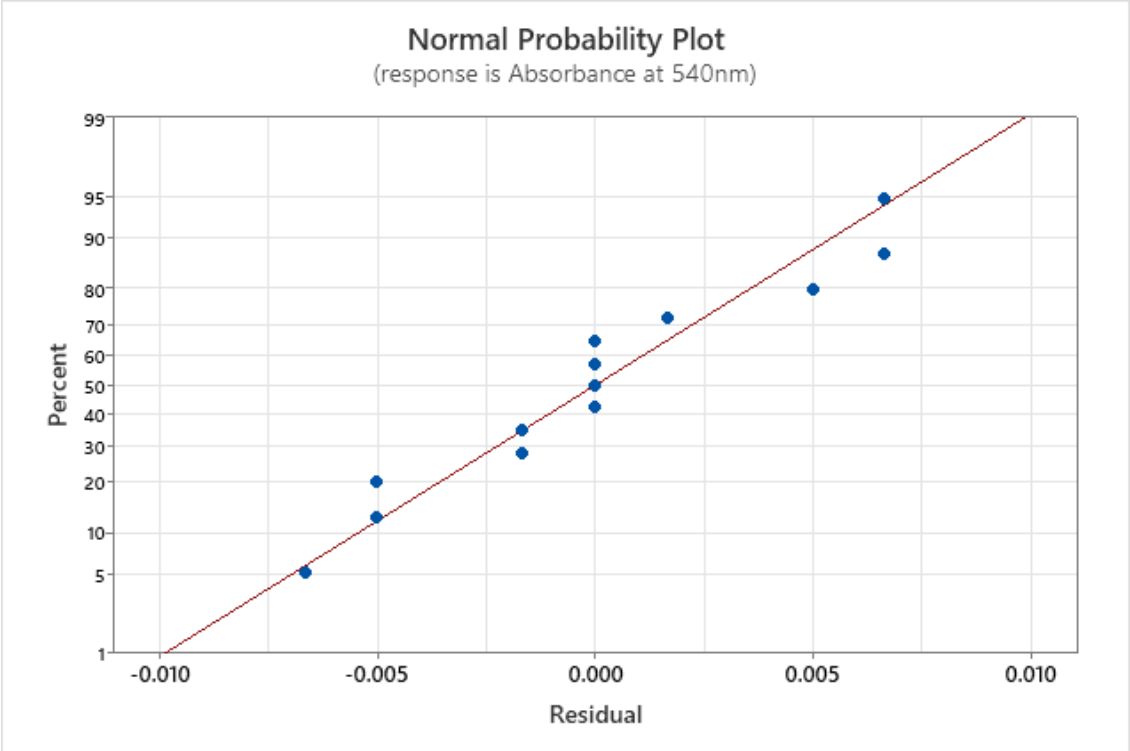
Normal Probability Plot
(response is Absorbance at 540nm)
Percent
99
95
90
80
70
60
50
40
30
20
10
5
1
-0.010
-0.005
0.000
0.005
0.010
Residual

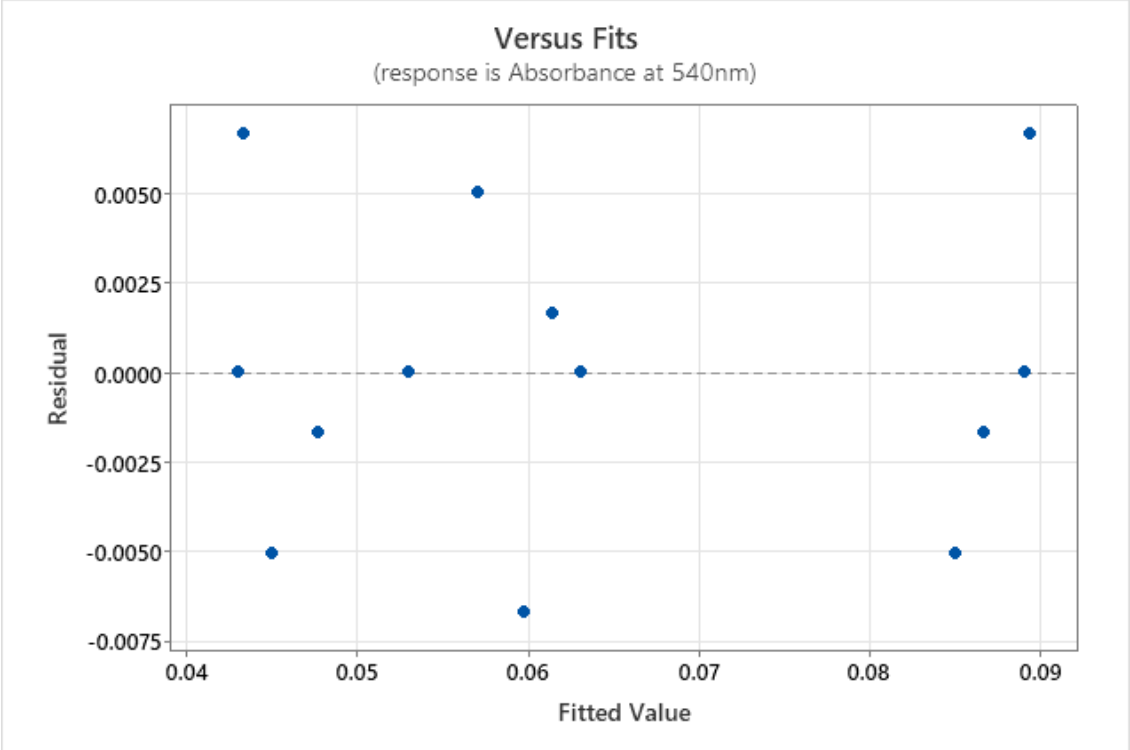
Versus Fits
(response is Absorbance at 540nm)
Residual
0.0050
0.0025
0.0000
-0.0025
-0.0050
-0.0075
0.04
0.05
0.06
0.07
0.08
0.09
Fitted Value

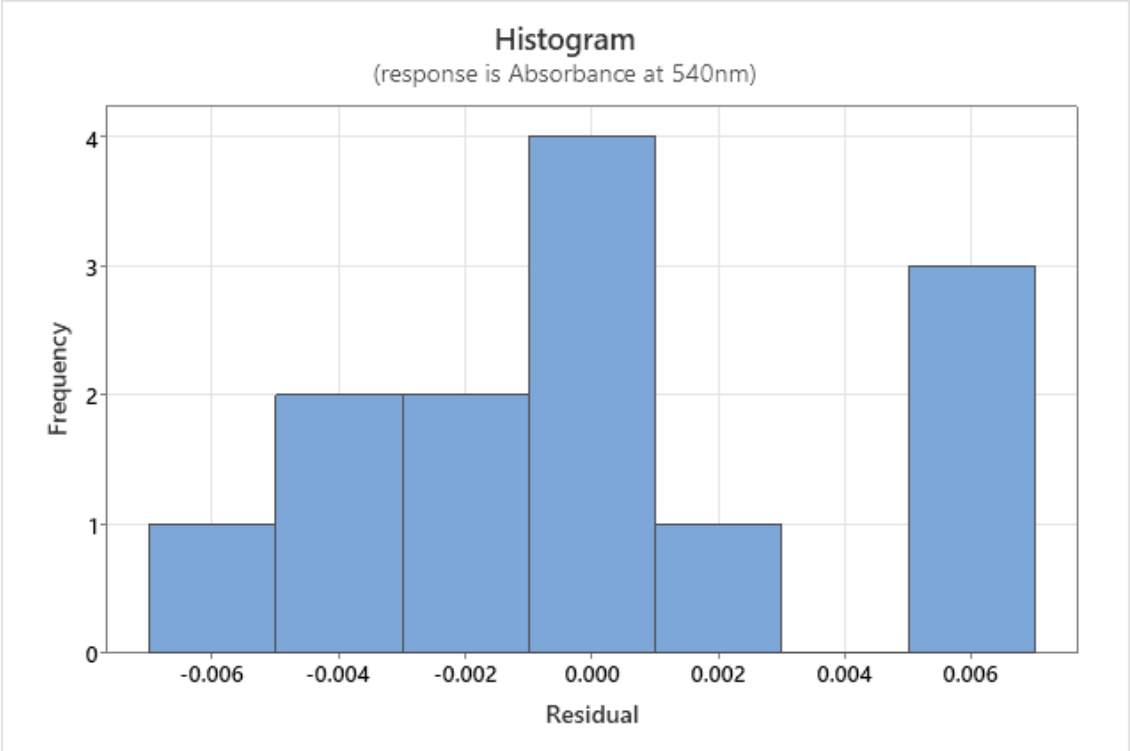
Histogram
(response is Absorbance at 540nm)
Frequency
4
3
2
1
0
-0.006
-0.004
-0.002
0.000
0.002
0.004
0.006
Residual

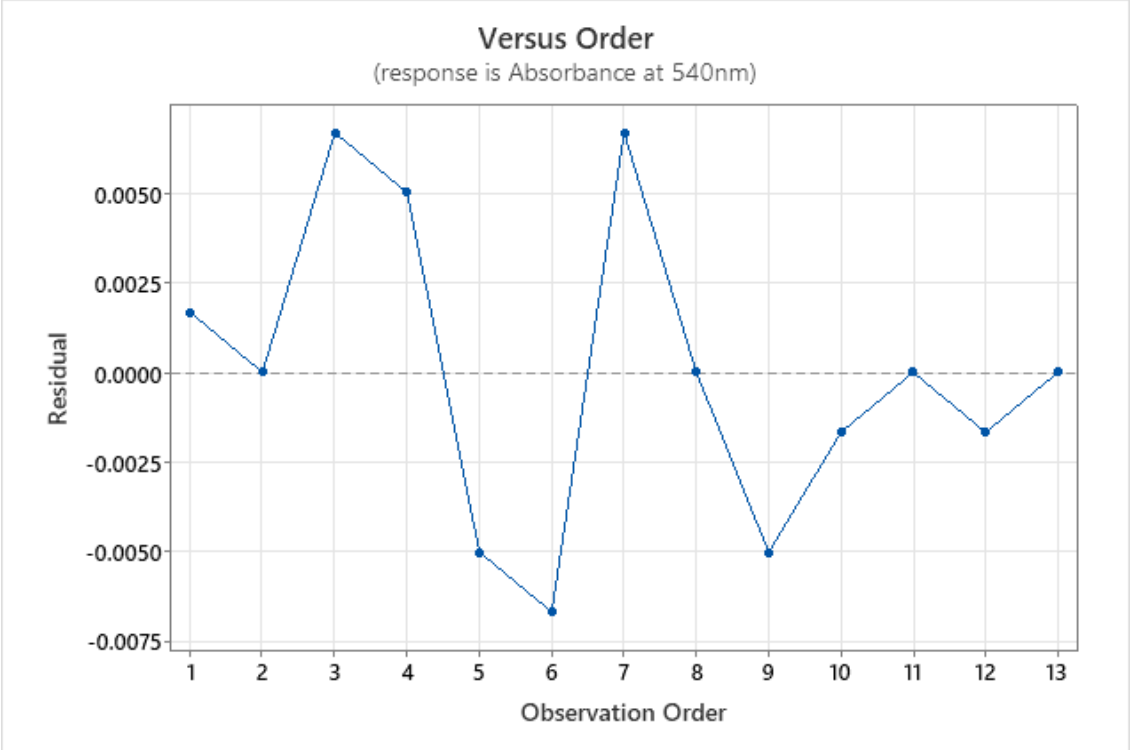

Response surface methodology results of *Proteus mirabilis*:

Response Surface Regression: Enzyme activity (Units) versus Inoculum size, pH

Coded Coefficients

Term	Coef	SE Coef	T-Value	P-Value	VIF
Constant	2.619	0.475	5.51	0.001	
Inoculum size	0.859	0.389	2.21	0.063	2.25
pH	0.598	0.308	1.94	0.093	1.28
Inoculum size*Inoculum size	-0.332	0.256	-1.30	0.236	2.35
pH*pH	-0.508	0.195	-2.61	0.035	1.07
Inoculum size*pH	0.426	0.436	0.98	0.360	1.28

Model Summary

S	R-sq	R-sq(adj)	R-sq(pred)
0.940393	69.07%	46.97%	0.00%

Analysis of Variance

Source	DF	Adj SS	Adj MS	F-Value	P-Value
Model	5	13.8228	2.7646	3.13	0.085
Linear	2	7.6594	3.8297	4.33	0.060
Inoculum size	1	4.3162	4.3162	4.88	0.063
pH	1	3.3432	3.3432	3.78	0.093
Square	2	6.4788	3.2394	3.66	0.082
Inoculum size*Inoculum size	1	1.4855	1.4855	1.68	0.236

pH*pH	1	6.0195	6.0195	6.81	0.035
2-Way Interaction	1	0.8476	0.8476	0.96	0.360
Inoculum size*pH	1	0.8476	0.8476	0.96	0.360
Error	7	6.1904	0.8843		
Lack-of-Fit	3	5.7255	1.9085	16.42	0.010
Pure Error	4	0.4649	0.1162		
Total	12	20.0131			

Regression Equation in Uncoded Units

Enzyme activity (Units) = -24.3 - 0.97 Inoculum size + 7.17 pH
- 0.186 Inoculum size*Inoculum size - 0.508 pH*pH
+ 0.319 Inoculum size*pH

Fits and Diagnostics for Unusual Observations

Obs	Enzyme activity (Units)	Fit	Resid	Std Resid	
3	2.716	1.092	1.624	2.17	R
8	0.014	0.850	-0.836	-2.07	R

R Large residual

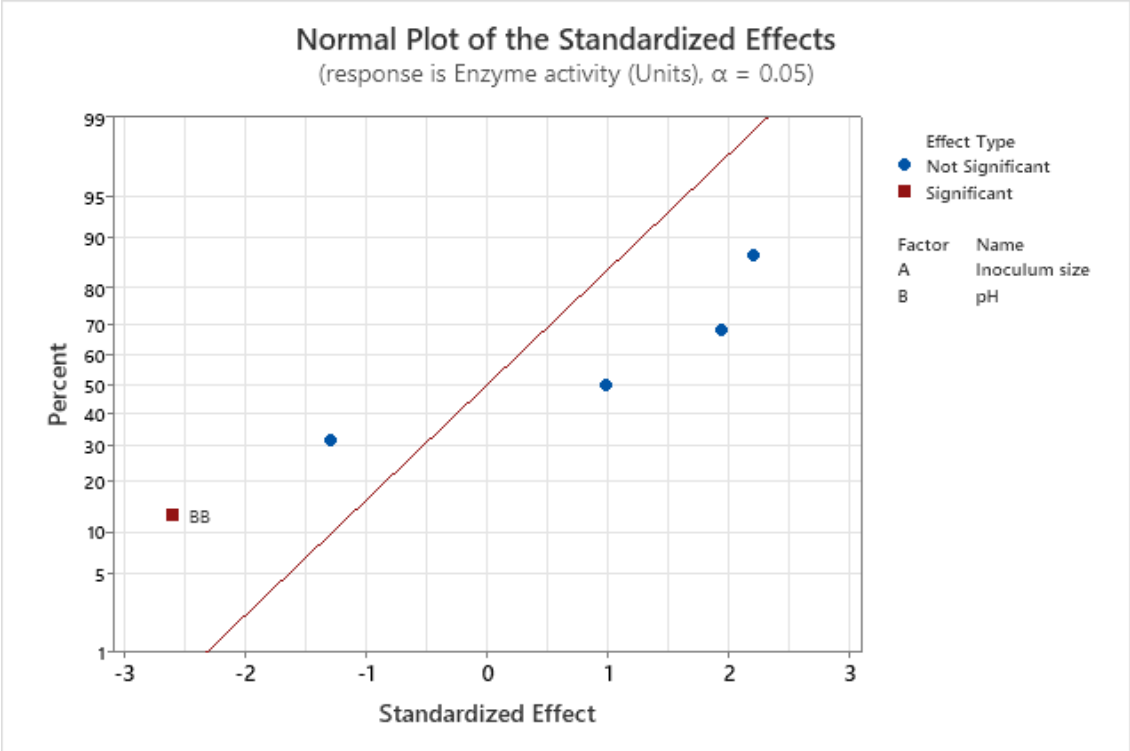

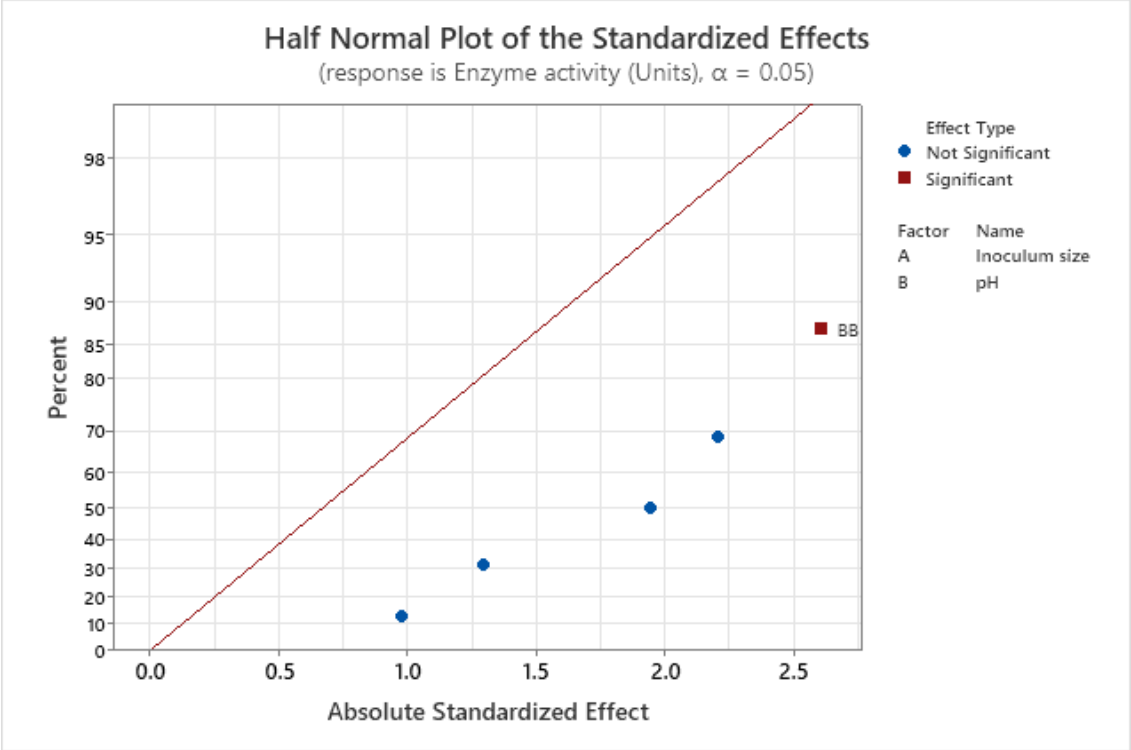
Half Normal Plot of the Standardized Effects
(response is Enzyme activity (Units), α = 0.05)
Percent
98
95
90
85
80
70
60
50
40
30
20
10
0
0.0
0.5
1.0
1.5
2.0
2.5
Absolute Standardized Effect
BB
Effect Type
Not Significant
Significant
Factor Name
A Inoculum size
B pH

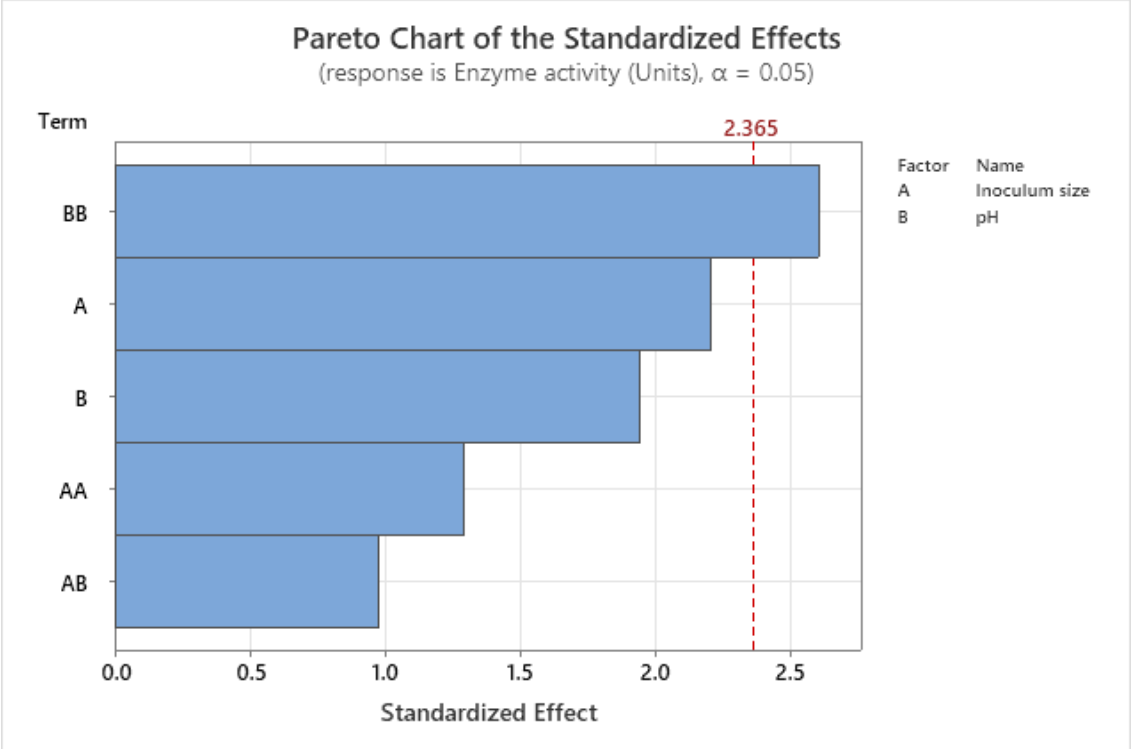
Pareto Chart of the Standardized Effects
(response is Enzyme activity (Units), α = 0.05)
Term
2.365
BB
A
B
AA
AB
0.0
0.5
1.0
1.5
2.0
2.5
Standardized Effect
Factor Name
A Inoculum size
B pH

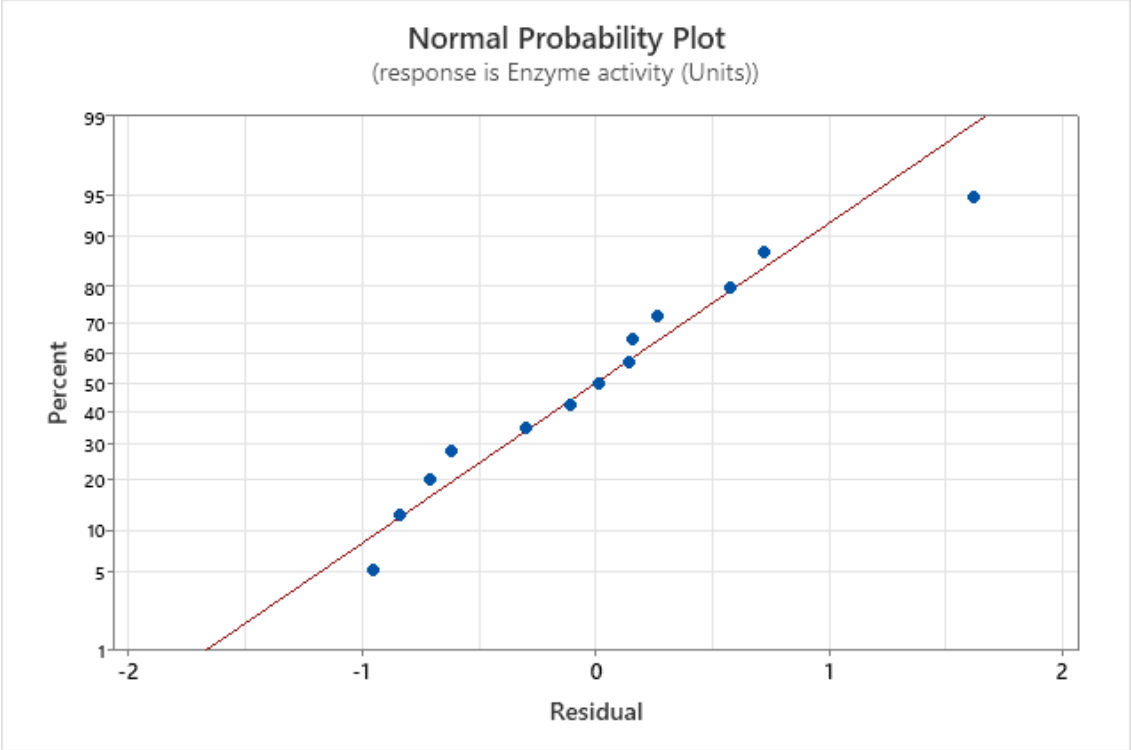
Normal Probability Plot
(response is Enzyme activity (Units))
Percent
99
95
90
80
70
60
50
40
30
20
10
5
1
-2
-1
0
1
2
Residual

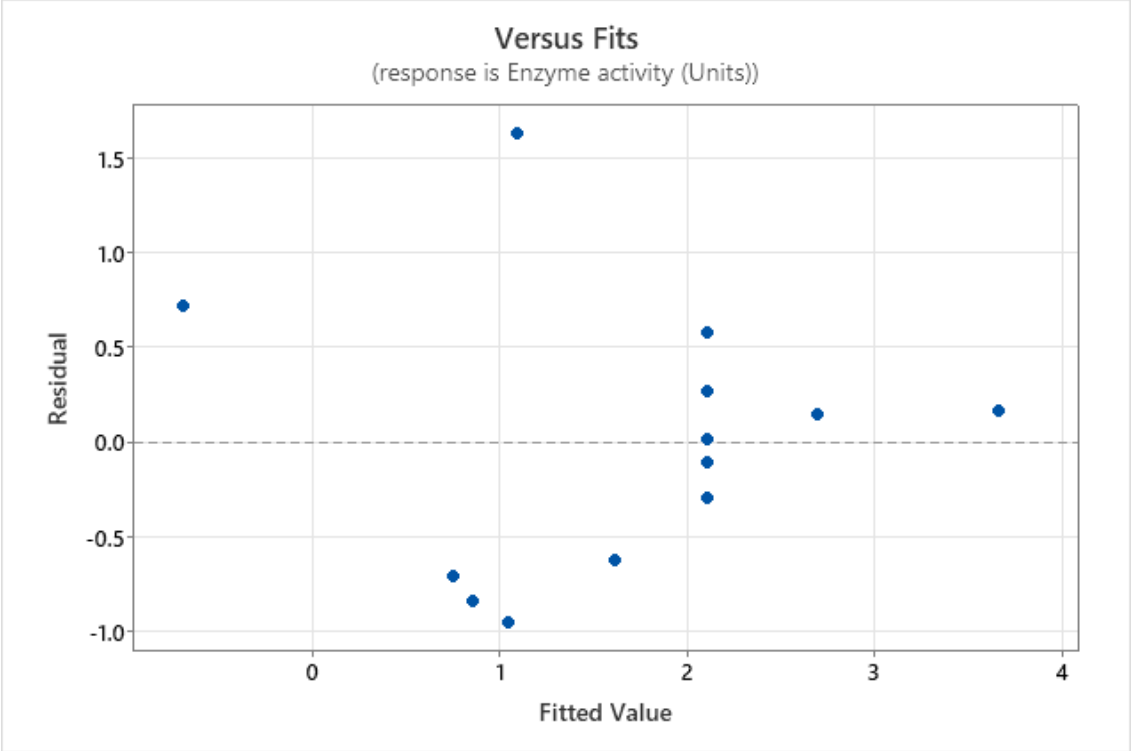
Versus Fits
(response is Enzyme activity (Units))
Residual
1.5
1.0
0.5
0.0
-0.5
-1.0
0
1
2
3
4
Fitted Value

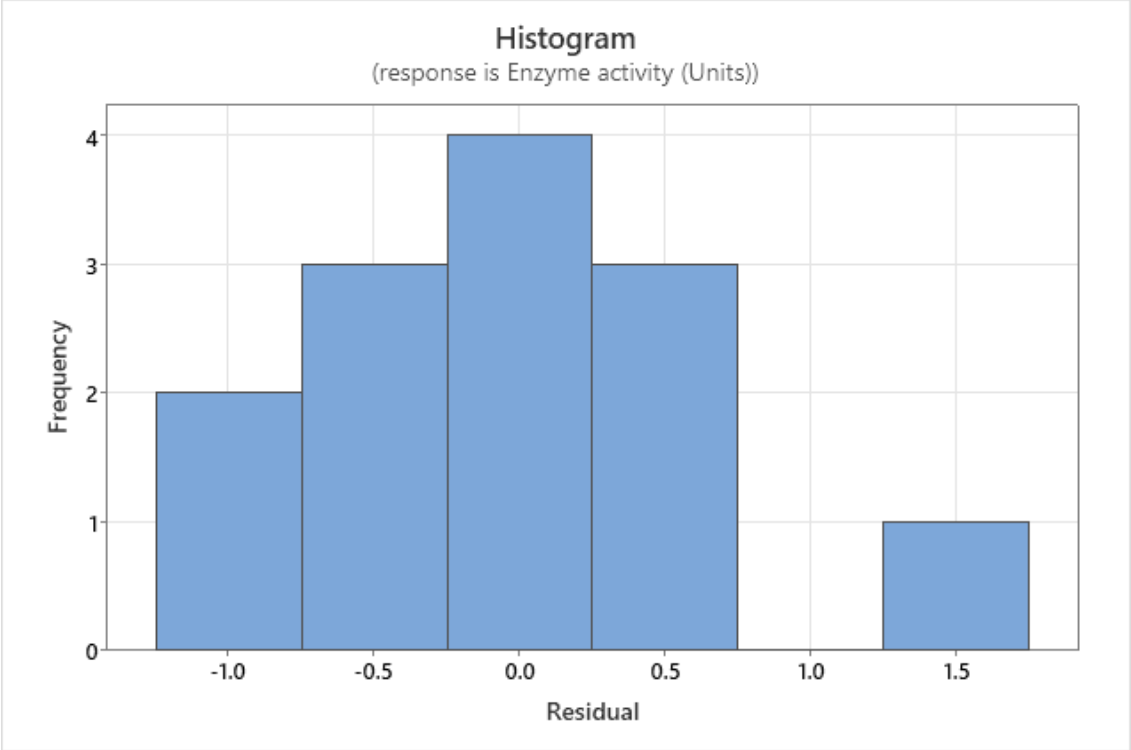
Histogram
(response is Enzyme activity (Units))
Frequency
Residual
0
1
2
3
4
-1.0
-0.5
0.0
0.5
1.0
1.5

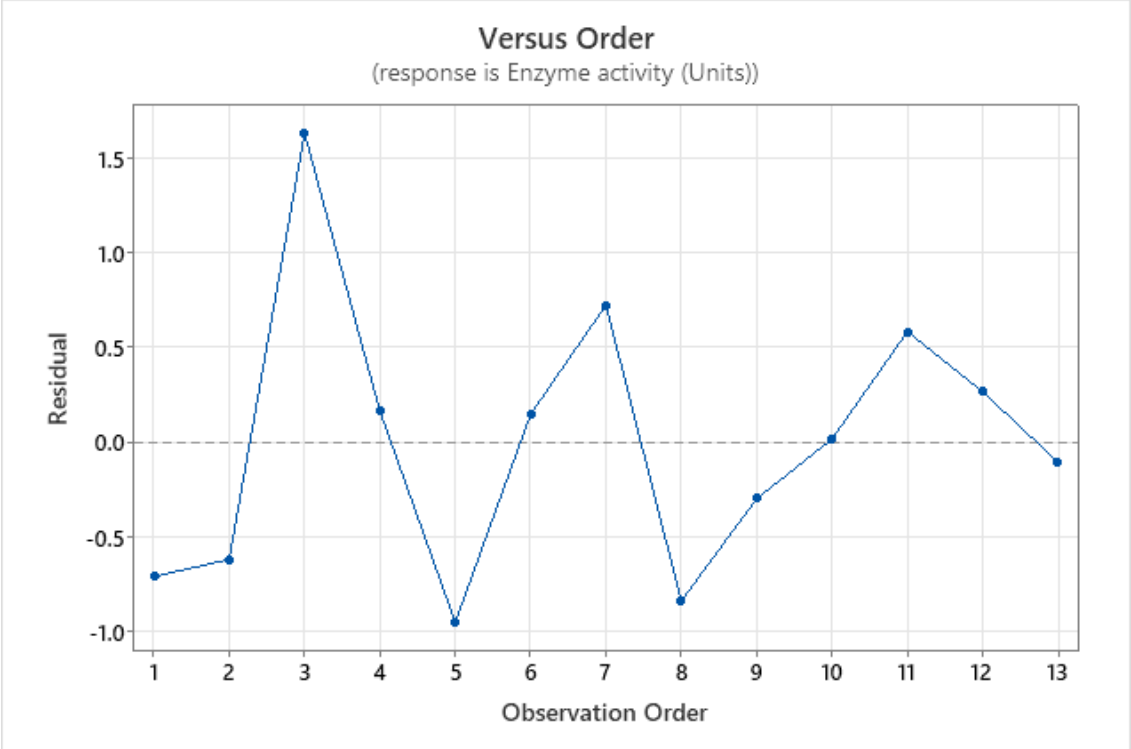
Versus Order
(response is Enzyme activity (Units))
Residual
Observation Order
1.5
1.0
0.5
0.0
-0.5
-1.0
1
2
3
4
5
6
7
8
9
10
11
12
13

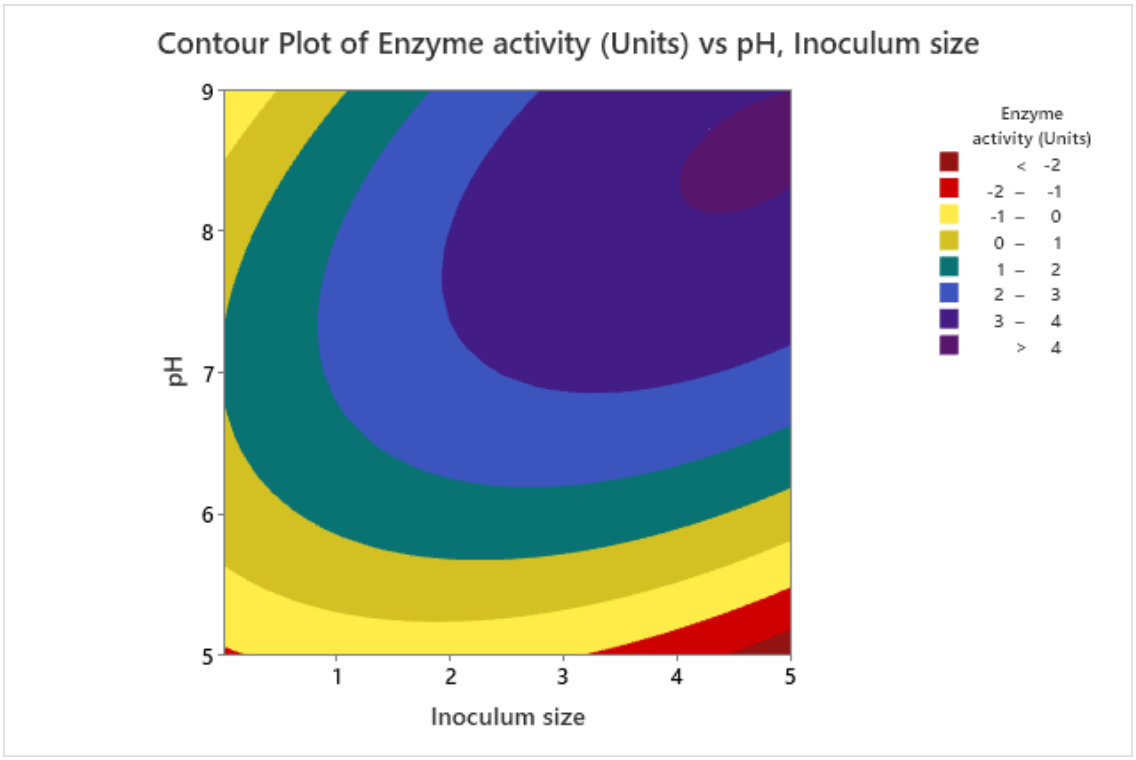
Contour Plot of Enzyme activity (Units) vs pH, Inoculum size
pH
Inoculum size
9
8
7
6
5
1
2
3
4
5
Enzyme activity (Units)
< -2
-2 – -1
-1 – 0
0 – 1
1 – 2
2 – 3
3 – 4
> 4

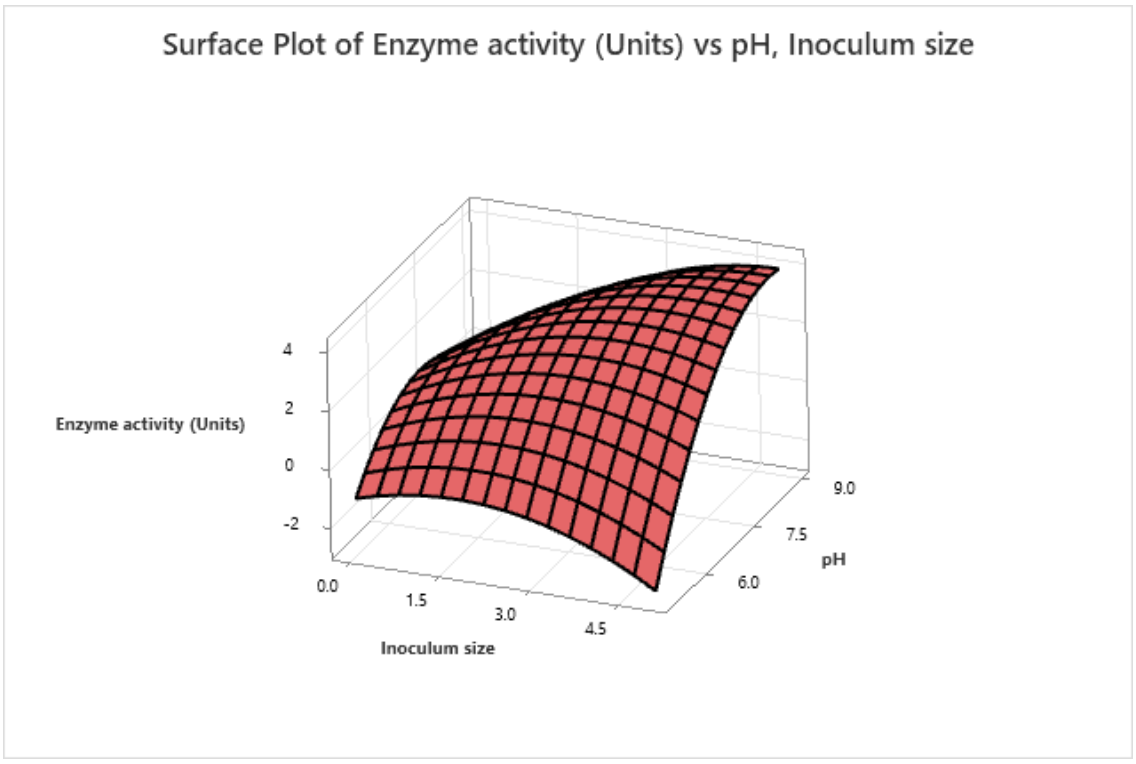
Surface Plot of Enzyme activity (Units) vs pH, Inoculum size
Enzyme activity (Units)
4
2
0
-2
0.0
1.5
3.0
4.5
Inoculum size
9.0
7.5
6.0
pH

Response surface methodology results of *Achromobacter denitrificans*:

Response Surface Regression: ENZYME ACTIVITY (UNITS) versus LBG, pH

Coded Coefficients

Term	Coef	SE Coef	T-Value	P-Value	VIF
Constant	1.933	0.553	3.50	0.010	
LBG	0.189	0.434	0.44	0.676	1.12
pH	0.509	0.378	1.34	0.221	1.00
LBG*LBG	-0.283	0.350	-0.81	0.445	1.21
pH*pH	-0.436	0.273	-1.60	0.154	1.08
LBG*pH	-0.237	0.655	-0.36	0.729	1.00

Model Summary

S	R-sq	R-sq(adj)	R-sq(pred)
1.31057	40.14%	0.00%	0.00%

Analysis of Variance

Source	DF	Adj SS	Adj MS	F-Value	P-Value
Model	5	8.0624	1.6125	0.94	0.510
Linear	2	3.4322	1.7161	1.00	0.415
LBG	1	0.3270	0.3270	0.19	0.676
pH	1	3.1052	3.1052	1.81	0.221
Square	2	4.6478	2.3239	1.35	0.319
LBG*LBG	1	1.1232	1.1232	0.65	0.445
pH*pH	1	4.3850	4.3850	2.55	0.154
2-Way Interaction	1	0.2240	0.2240	0.13	0.729
LBG*pH	1	0.2240	0.2240	0.13	0.729
Error	7	12.0232	1.7176		
Lack-of-Fit	3	8.4567	2.8189	3.16	0.148
Pure Error	4	3.5665	0.8916		
Total	12	20.0856			

Regression Equation in Uncoded Units

ENZYME ACTIVITY (UNITS) = -26.4 + 1.35 LBG + 6.97 pH - 0.0707 LBG*LBG - 0.436 pH*pH - 0.118 LBG*pH

Fits and Diagnostics for Unusual Observations

Obs	ENZYME ACTIVITY (UNITS)	Fit	Resid	Std Resid	
3	3.567	1.771	1.796	2.03	R

R Large residual

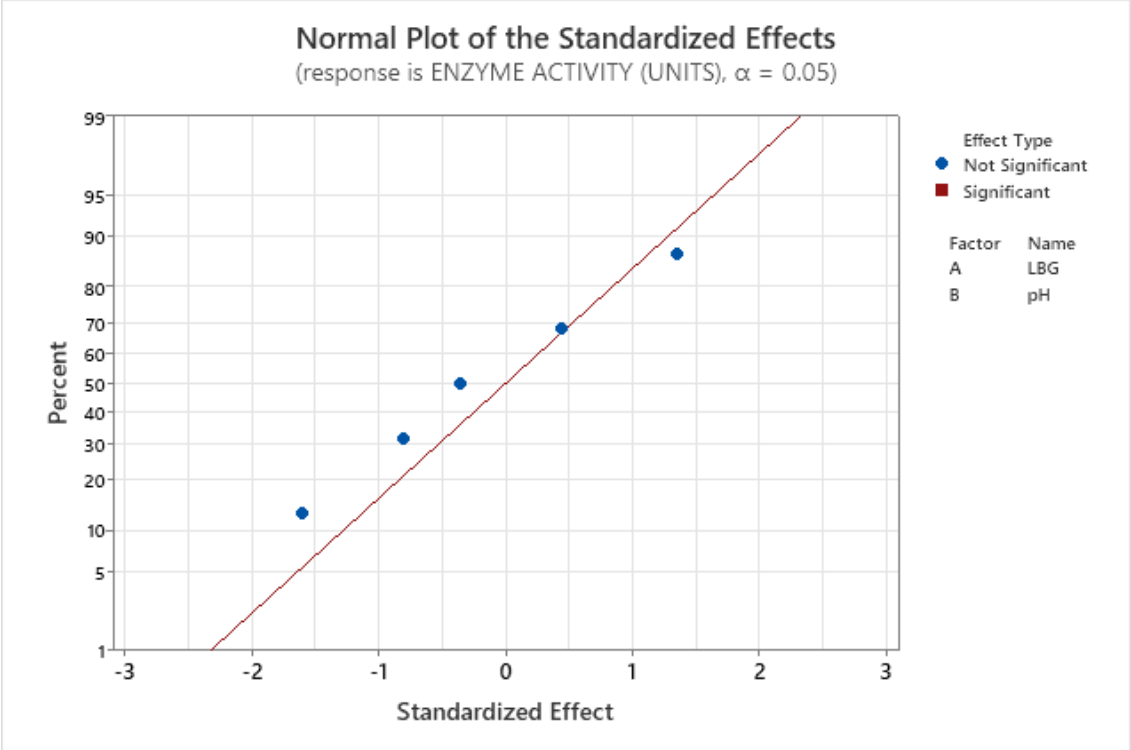
Normal Plot of the Standardized Effects
(response is ENZYME ACTIVITY (UNITS), α = 0.05)
Percent
99
95
90
80
70
60
50
40
30
20
10
5
1
-3
-2
-1
0
1
2
3
Standardized Effect
Effect Type
Not Significant
Significant
Factor Name
A LBG
B pH

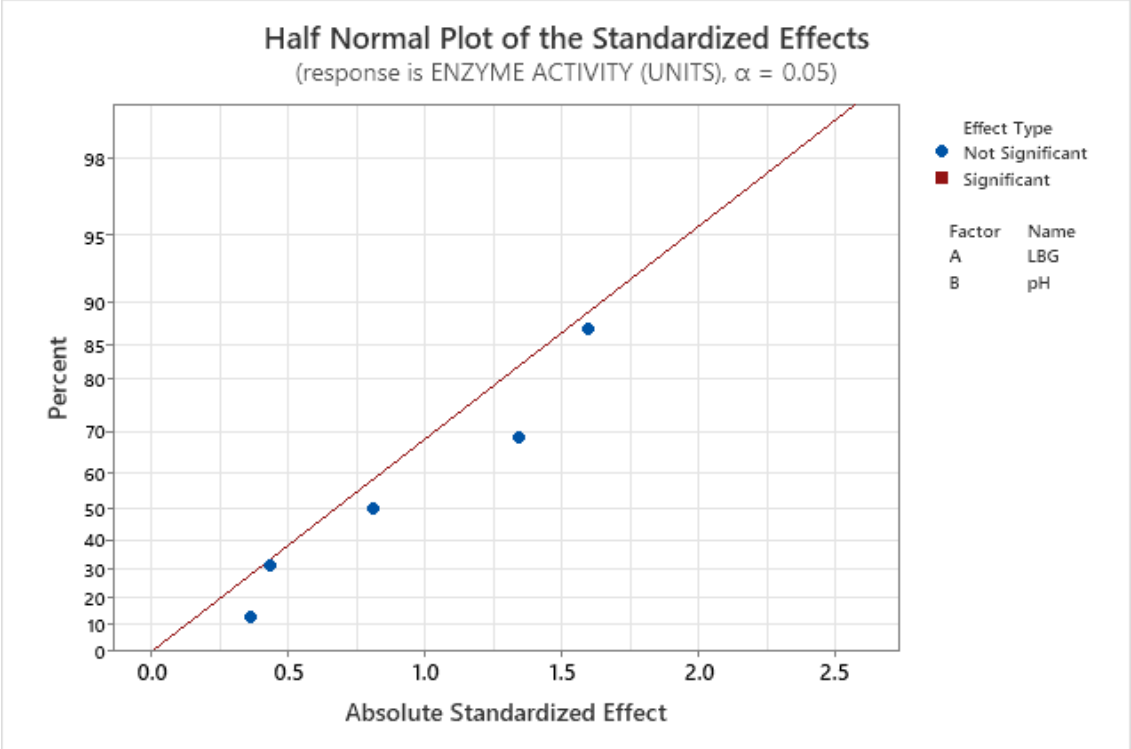
Half Normal Plot of the Standardized Effects
(response is ENZYME ACTIVITY (UNITS), α = 0.05)
Percent
98
95
90
85
80
70
60
50
40
30
20
10
0
0.0
0.5
1.0
1.5
2.0
2.5
Absolute Standardized Effect
Effect Type
Not Significant
Significant
Factor Name
A LBG
B pH

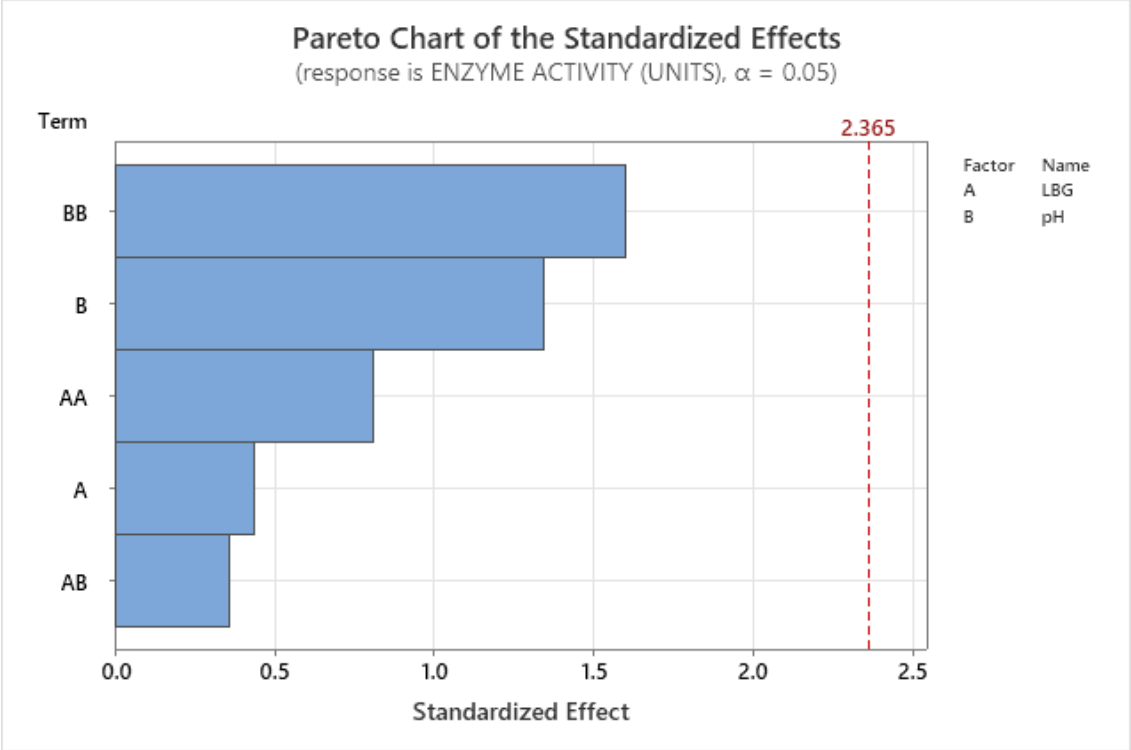
Pareto Chart of the Standardized Effects
(response is ENZYME ACTIVITY (UNITS), α = 0.05)
Term
2.365
BB
B
AA
A
AB
0.0
0.5
1.0
1.5
2.0
2.5
Standardized Effect
Factor Name
A LBG
B pH

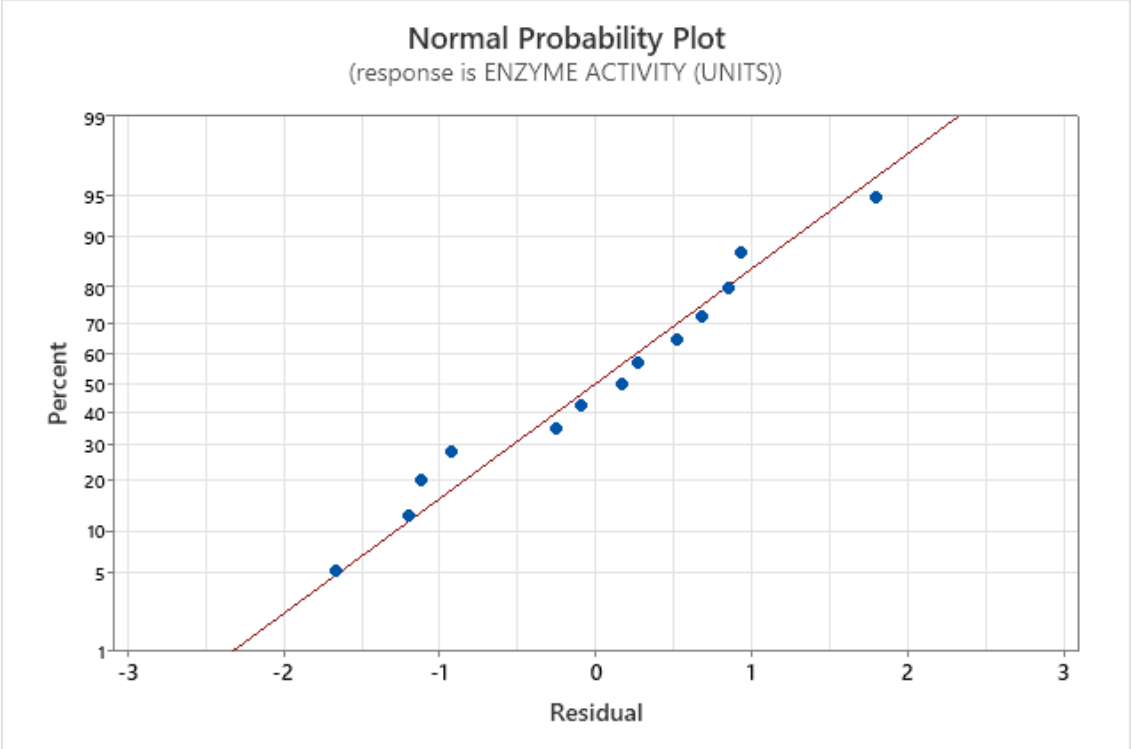
Normal Probability Plot
(response is ENZYME ACTIVITY (UNITS))
Percent
99
95
90
80
70
60
50
40
30
20
10
5
1
-3
-2
-1
0
1
2
3
Residual

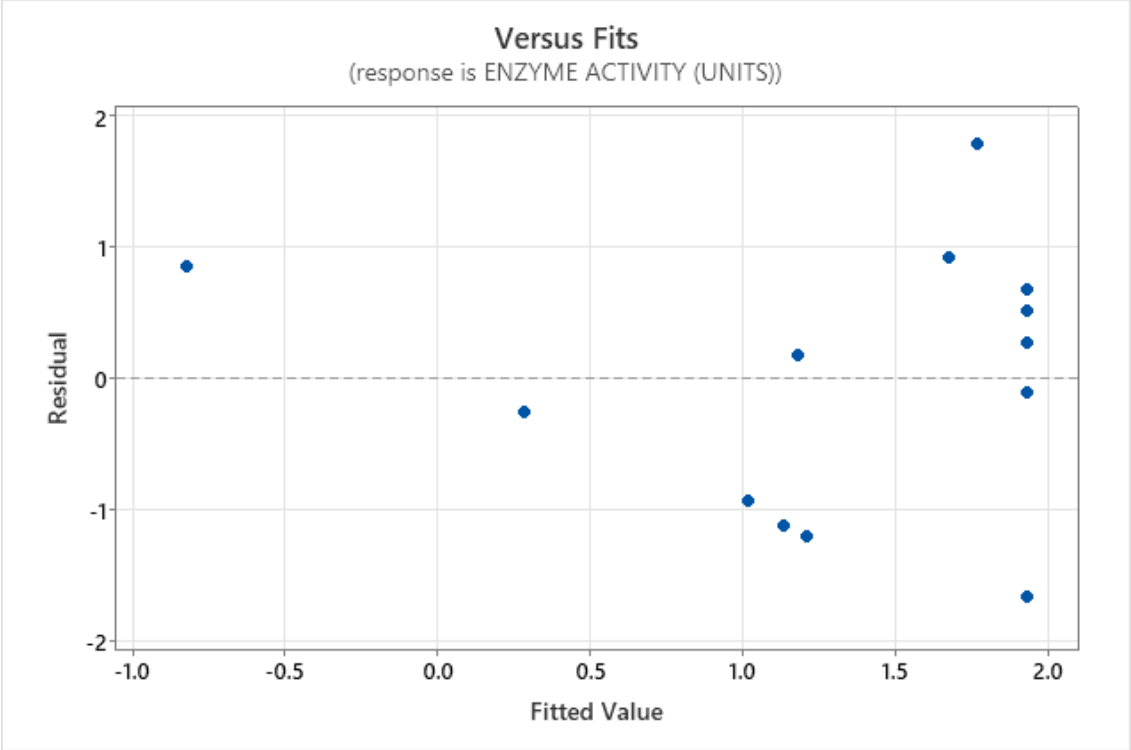
Versus Fits
(response is ENZYME ACTIVITY (UNITS))
Residual
Fitted Value
2
1
0
-1
-2
-1.0
-0.5
0.0
0.5
1.0
1.5
2.0

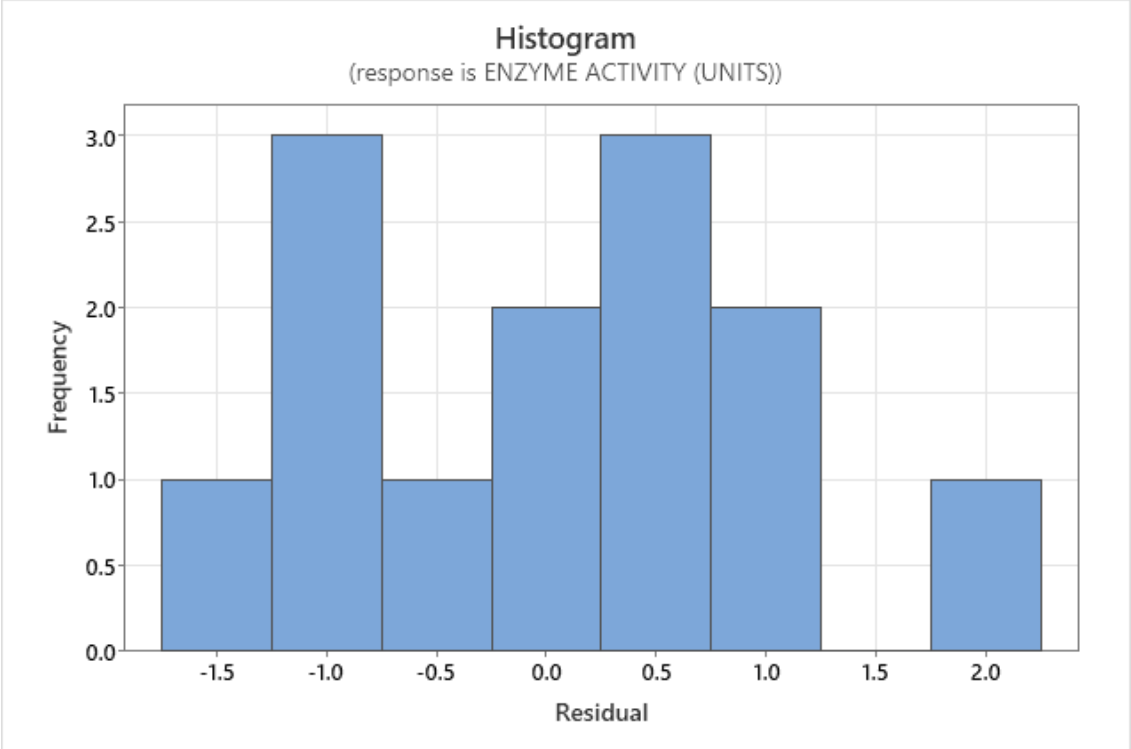
Histogram
(response is ENZYME ACTIVITY (UNITS))
Frequency
Residual
3.0
2.5
2.0
1.5
1.0
0.5
0.0
-1.5
-1.0
-0.5
0.0
0.5
1.0
1.5
2.0

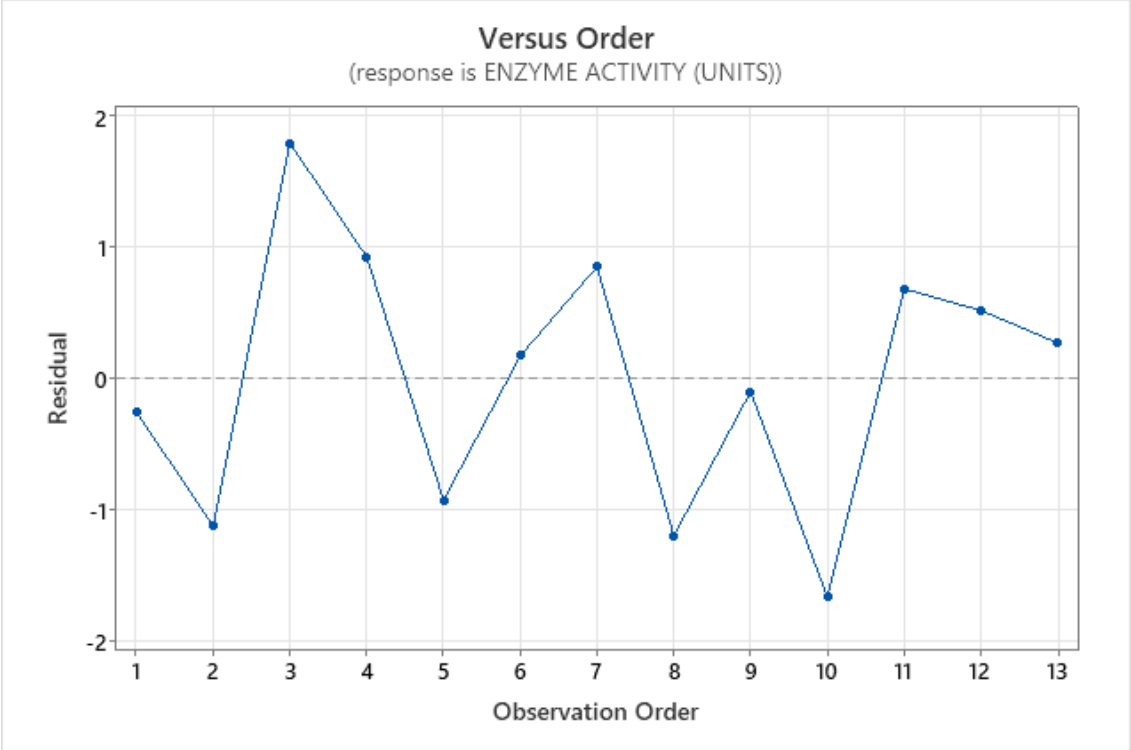

WORKSHEET 1

Contour Plot of ENZYME ACTIVITY (UNITS) vs pH, LBG

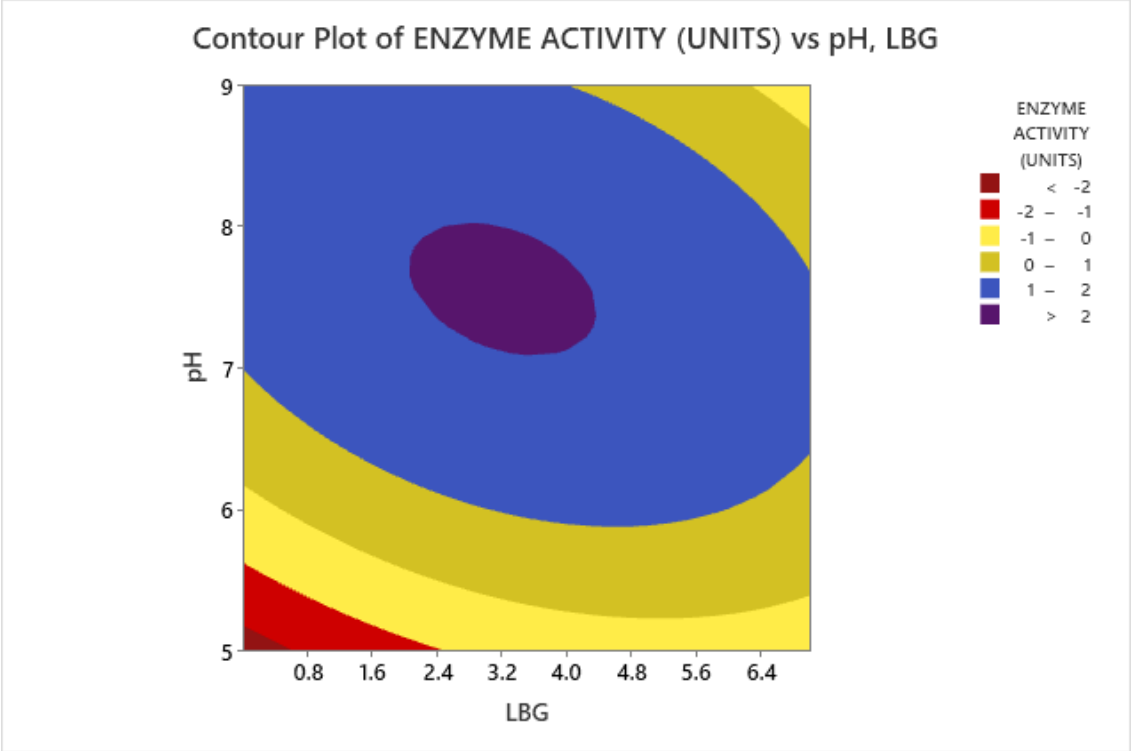

WORKSHEET 1

Surface Plot of ENZYME ACTIVITY (UNITS) vs pH, LBG

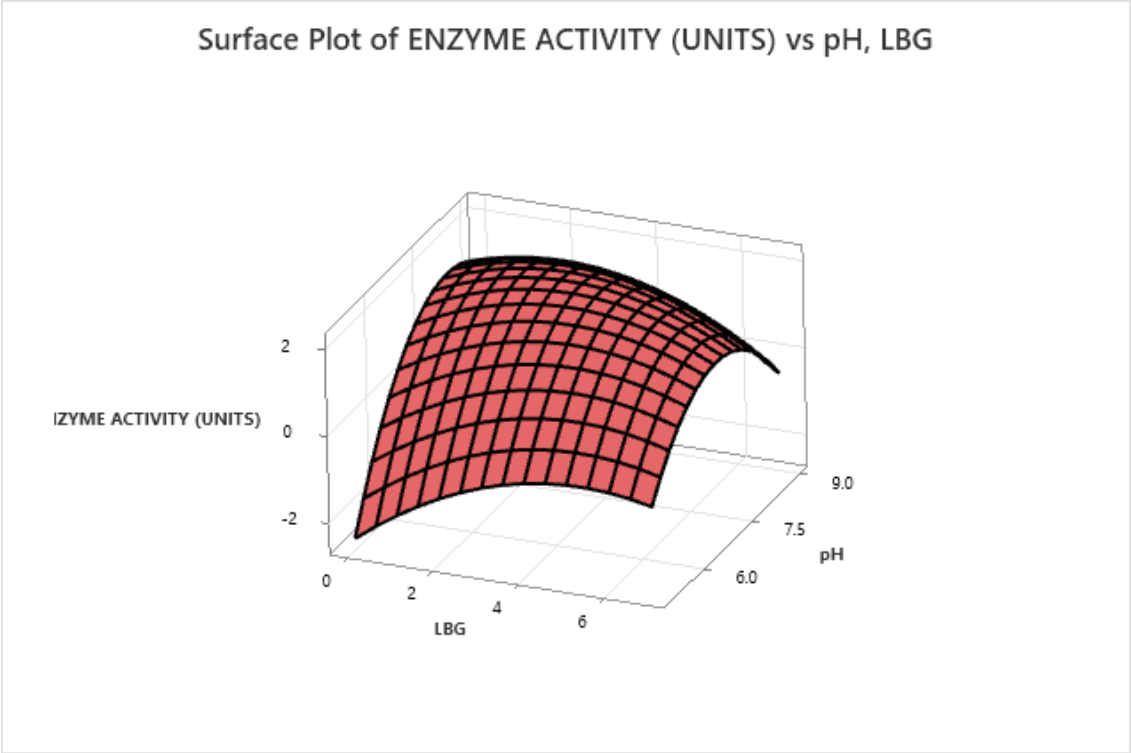

Purification of mannanase from *Proteus mirabilis* and *Achromobacter denitrificans*

PURIFICATION chart of mannanase extracted from *Proteus mirabilis*

Step	Volume(ml)	Total protein (mg)	Total activity (units)	Specific activity (units/mg)	Fold purification	Yield %
Crude enzyme	160	5834.409	688.88	0.118	1	100
Ammonium salt precipitation	5	127.89	593.56	4.64	39.31	86.16

PURIFICATION chart of mannanase extracted from *Achromobacter denitrificans*

step	Volume(ml)	Total protein (mg)	Total activity (units)	Specific activity (units/mg)	Fold purification	Yield %
Crude enzyme	160	5318.28	622.4	0.117	1	100
Ammonium salt precipitation	5	115.92	583.69	5.035	43.02	93.78

Second generation ethanol production

500 U of β-mannanase were isolated from *Proteus mirabilis* production medium and introduced to YPA fermentation media containing 5 g/L of 1,4-β-d-mannan. *Saccharomyces cerevisiae* fermented this medium, producing 1.367 g/L of ethanol in a 24-hour period. While 5, g/L of 1,4-β-d-mannan was present in the YPA fermentation medium, β-mannanase (500 U) was isolated from the production media of *Achromobacter denitrificans*. *Saccharomyces cerevisiae* fermented this medium, producing 1.642 g/L of ethanol in under 24 hours.

CONCLUSION

- *Proteus mirabilis* and *Achromobacter dinitrificans* have been isolated and shown the ability to produce mannanse.
- Proteus mirabilis has been first time reported to produce mannase.
- *Proteus mirabilis* and *Achromobactor dinitrificans* mannase production have been optimized using Plackett Burman and RSM.
- This mannanase was used to saccharify plant mannan and used this saccharified material to ferment into ethanol.

REFERENCE

- Kraan, S. (2012). Algal Polysaccharides, Novel Applications and Outlook. InTech. doi: 10.5772/51572
- Yasar Yildiz, S., & Toksoy Oner, E. (2014). Mannan as a Promising Bioactive Material for Drug Nanocarrier Systems. InTech. doi: 10.5772/58413
- Voiniciuc, C. (2022), Modern mannan: a hemicellulose's journey. New Phytol, 234: 1175-1184. https://doi.org/10.1111/nph.18091
- Mafa, M. S., & Malgas, S. (2023). Towards an understanding of the enzymatic degradation of complex plant mannan structures. World Journal of Microbiology and Biotechnology, 39(11), 302.
- Mpofu, C. M., Campbell, B. J., Subramanian, S., Marshall–Clarke, S., Hart, C. A., Cross, A., ... & Rhodes, J. M. (2007). Microbial mannan inhibits bacterial killing by macrophages: a possible pathogenic mechanism for Crohn's disease. Gastroenterology, 133(5), 1487-1498.
- Van den Abbeele, P., Duysburgh, C., Rakebrandt, M., & Marzorati, M. (2020). Dried yeast cell walls high in beta-glucan and mannan-oligosaccharides positively affect microbial composition and activity in the canine gastrointestinal tract in vitro. Journal of Animal Science, 98(6), skaa173.
- Chauhan, P. S., Puri, N., Sharma, P., and Gupta, N. (2012). Mannanases: microbial sources, production, properties and potential biotechnological applications. Appl. Microbiol. Biotechnol. 93, 1817–1830. doi: 10.1007/s00253-012-3887-5
- Malgas, S., van Dyk, J. S., and Pletschke, B. I. (2015). A review of the enzymatic hydrolysis of mannans and synergistic interactions between b-mannanase, b-mannosidase and a-galactosidase. World J. Microbiol. Biotechnol. 31, 1167–1175. doi: 10.1007/s11274-015-1878-2
- Morreira, L. (2008). An overview of mannan structure and mannan-degrading enzyme systems. Appl.Microbiol. Biotechnol. 79, 165–178. doi: 10.1007/s00253-008-1423-4
- Songsiriritthigul, C., Lapboonrueng, S., Roytrakul, S., Haltrich, D., and Yamabhai, M. (2011). Crystallization and preliminary crystallographic analysis of b-mannanase from *Bacillus licheniformis*. Acta Cryst. Sec. F Struct. Biol. Cryst. Commun. 67, 217–220. doi: 10.1107/s1744309110049067

- Dawood A and Ma K (2020) Applications of Microbial -Mannanases. Front. Bioeng. Biotechnol. 8:598630. doi: 10.3389/fbioe.2020.598630
- Latham, R., Williams, M., Walters, H., Carter, B., and Lee, J. (2018). Efficacy of b-mannanase on broiler growth performance and energy utilization in the presence of increasing dietary galactomannan. Poult. Sci. 97, 549–556. doi:10.3382/ps/pex309
- Mojsov, K. (2011). "Application of enzymes in the textile industry: a review," in Proceedings of the II International Congress "Engineering, Ecology and Materials in the Processing Industry", (Jahorina), 230–239.
- Zhang, C. (2019). Lignocellulosic Ethanol: Technology and Economics, Alcohol Fuels-Current Technologies and Future Prospect. London: IntechOpen.
- Galli, S. J., and Tsai, M. (2012). IgE and mast cells in allergic disease. Nat. Med. 18, 693–704. doi: 10.1038/nm.2755
- Yang, M., Cai, J., Wang, C., Du, X., and Lin, J. (2017). Characterization of endo-b-mannanase from Enterobacter ludwigii MY271 and application in pulp industry. Bioprocess Biosyst. Eng. 40, 35–43. doi: 10.1007/s00449-016-1672-z
- Khampheng Phothichitto, Sunee Nitisinprasert and Suttipun Keawsompong, Isolation, Screening and Identification of Mannanase Producing Microorganisms, Kasetsart J. (Nat. Sci.) 40 (Suppl.): 26 - 38 (2006)
- Rosariastuti, R., Sutami, Sumani, & Hartati, S.Y. (2022). Analysis of bacterial community from the rhizosphere of shallots (Allium ascalonicum L.) in Brebes, Central Java, using Next Generation Sequencing (NGS) approach. IOP Conference Series: Earth and Environmental Science, 1114.
- Abe J, Hossain ZM, Hizukuri S (1994) Isolation of b-mannanase producing microorganisms. J Ferment Bioeng 3:259–261.
- Surachai Rattanasuk and Mareina Ketudat-Cairns, Chryseobacterium indologenes, novel mannanase-producing bacteria, Songklanakarin J. Sci. Technol. 31 (4), Jul. - Aug. 2009.
- Lifeng Cheng, Shengwen Duan, Xiangyuan Feng, Ke Zheng, Qi Yang, and Zhengchu Liu, Purification and Characterization of a Thermostable β-Mannanase from Bacillus subtilis BE-91: Potential Application in Inflammatory Diseases, BioMed Research International Volume 2016, Article ID 6380147, 7 pages http://dx.doi.org/10.1155/2016/6380147

- Sudathip Titapoka, Suttipun Keawsompong, Dietmar Haltrich and Sunee Nitisinprasert, Selection and characterization of mannanase-producing bacteria useful for the formation of prebiotic manno-oligosaccharides from copra meal, World J Microbiol Biotechnol (2008) 24:1425–1433, DOI 10.1007/s11274-007-9627-9
- Altschul, Stephen F., Warren Gish, Webb Miller, Eugene W. Myers, and David J. Lipman. 1990. "Basic Local Alignment Search Tool." Journal of Molecular Biology 215 (3): 403–10. https://doi.org/10.1016/s0022-2836(05)80360-2.
- Edgar, Robert C. 2004. BMC Bioinformatics 5 (1): 113. https://doi.org/10.1186/1471-2105-5-113.
- Martin, Kendall J, and Paul T Rygiewicz. 2005. BMC Microbiology 5 (1): 28. https://doi.org/10.1186/1471-2180-5-28.
- Quast, Christian, Elmar Pruesse, Pelin Yilmaz, Jan Gerken, Timmy Schweer, Pablo Yarza, Jörg Peplies, and Frank Oliver Glöckner. 2012. "The SILVA Ribosomal RNA Gene Database Project: Improved Data Processing and Web-Based Tools." Nucleic Acids Research 41 (D1): D590–96. https://doi.org/10.1093/nar/gks1219 .
- Tamura, Koichiro, Glen Stecher, and Sudhir Kumar. 2021. "MEGA11: Molecular Evolutionary Genetics Analysis Version 11." Edited by Fabia Ursula Battistuzzi. Molecular Biology and Evolution 38 (7): 3022–27. https://doi.org/10.1093/molbev/msab120.
- Elsayed, Elsayed Ahmed, Ahmed Abdelwahed, Nayera, Medium Optimization by Response Surface Methodology for Improved Cholesterol Oxidase Production by a Newly Isolated Streptomyces rochei NAM-19 Strain, BioMed Research International, 2020, 1870807, 13 pages, 2020. https://doi.org/10.1155/2020/1870807
- Katoch, R. (2011). Analytical techniques in biochemistry and molecular biology. Springer Science & Business Media.
- Ishii, J., Okazaki, F., Djohan, A. C., Hara, K. Y., Asai-Nakashima, N., Teramura, H., ... & Kondo, A. (2016). From mannan to bioethanol: cell surface co-display of β-mannanase and β-mannosidase on yeast Saccharomyces cerevisiae. Biotechnology for Biofuels, 9, 1-15.